New Aspects of Invasive Growth Regulation Identified by Functional Profiling of MAPK Pathway Targets in *Saccharomyces cerevisiae*

Matthew D. Vandermeulen and Paul J. Cullen[1]
Department of Biological Sciences, University at Buffalo, New York 14260-1300
ORCID ID: 0000-0002-6703-1480 (P.J.C.)

ABSTRACT MAPK pathways are drivers of morphogenesis and stress responses in eukaryotes. A major function of MAPK pathways is the transcriptional induction of target genes, which produce proteins that collectively generate a cellular response. One approach to comprehensively understand how MAPK pathways regulate cellular responses is to characterize the individual functions of their transcriptional targets. Here, by examining uncharacterized targets of the MAPK pathway that positively regulates filamentous growth in *Saccharomyces cerevisiae* (fMAPK pathway), we identified a new role for the pathway in negatively regulating invasive growth. Specifically, four targets were identified that had an inhibitory role in invasive growth: *RPI1*, *RGD2*, *TIP1*, and *NFG1*/*YLR042c*. *NFG1* was a highly induced unknown open reading frame that negatively regulated the filamentous growth MAPK pathway. We also identified *SFG1*, which encodes a transcription factor, as a target of the fMAPK pathway. Sfg1p promoted cell adhesion independently from the fMAPK pathway target and major cell adhesion flocculin Flo11p, by repressing genes encoding presumptive cell-wall-degrading enzymes. Sfg1p also contributed to *FLO11* expression. Sfg1p and Flo11p regulated different aspects of cell adhesion, and their roles varied based on the environment. Sfg1p also induced an elongated cell morphology, presumably through a cell-cycle delay. Thus, the fMAPK pathway coordinates positive and negative regulatory proteins to fine-tune filamentous growth resulting in a nuanced response. Functional analysis of other pathways' targets may lead to a more comprehensive understanding of how signaling cascades generate biological responses.

KEYWORDS filamentous growth; transcription; expression profiling; fungal pathogens; adhesion

SIGNAL transduction pathways mediate cellular responses, which can include the response to stress, cell differentiation, and morphogenetic changes. One type of signaling pathway that functions in eukaryotes as a driver of development and stress responses are mitogen-activated protein kinase (MAPK) pathways, which regulate transcription factors that modify gene expression to induce a cellular response (Seger and Krebs 1995; Madhani *et al.* 1999; Chang and Karin 2001; Zeitlinger *et al.* 2003; Seger 2010; Morrison 2012). Because transcription factors can have many transcriptional targets, the individual functions of all targets must be considered to understand the complete phenotype of a signaling pathway. Thus, characterizing the transcriptional targets of a MAPK pathway may lead to new insights into the regulation of biological responses.

In the budding yeast *Saccharomyces cerevisiae*, the filamentous growth MAPK (fMAPK) pathway is one of multiple pathways that regulates the cellular response to nutrient limitation known as filamentous growth (Carlson *et al.* 1981; Gimeno *et al.* 1992; Lorenz and Heitman 1998; Pan and Heitman 1999, 2000; Cullen and Sprague 2000, 2012; Crespo *et al.* 2002; Lamb and Mitchell 2003; Borneman *et al.* 2006; Chavel *et al.* 2010, 2014; González *et al.* 2017; Norman *et al.* 2018; Mutlu *et al.* 2019; Brito *et al.* 2020). Filamentous growth occurs in many fungal species, and, in pathogenic fungi, such as the human pathogen *Candida albicans*, it is critical for virulence, making filamentous growth an important aspect of fungal biology (Lo *et al.* 1997; Wendland 2001; Nobile *et al.* 2006; Sohn *et al.* 2006; Labbaoui *et al.*

doi: https://doi.org/10.1534/genetics.120.303369
Manuscript received May 20, 2020; accepted for publication July 7, 2020; published Early Online July 14, 2020.
Supplemental material available at figshare: https://doi.org/10.25386/genetics.12609710.
[1]Corresponding author: Department of Biological Sciences, State University of New York at Buffalo, 532 Cooke Hall, Buffalo, NY 14260-1300. E-mail: pjcullen@buffalo.edu

2017; Zhao *et al.* 2018; Brito *et al.* 2020). Filamentous growth involves a switch from yeast-form growth (round cell morphology) to filamentous-form growth, where cells produce filament-like structures. The filament-like structures result from three major changes to the cell: an increase in cell length, a reorganization of cell polarity, and increased cell-to-cell adhesion (Roberts and Fink 1994; Cullen and Sprague 2012). Filamentous growth causes cells to invade into substrates, a behavior called invasive growth (Roberts and Fink 1994). Invasive growth is presumed to be a scavenging response for cells to search for nutrients because it is mainly induced by nutrient limitation, such as fermentable carbon source (Cullen and Sprague 2000, 2012) and nitrogen (Gimeno *et al.* 1992) limitation. It can also be induced by high cell density through quorum sensing molecules (Chen and Fink 2006; González *et al.* 2017; Lenhart *et al.* 2019). When cells adhere and invade together in high cell density, they can form a gouge into surfaces, which is called aggregate invasive growth (Chow *et al.* 2019a).

The fMAPK pathway controls the activity of transcription factors that includes Ste12p and Tec1p [Figure 1A, (Gimeno *et al.* 1992; Gimeno and Fink 1994; Borneman *et al.* 2006; Heise *et al.* 2010; Cullen and Sprague 2012; van der Felden *et al.* 2014)]. These proteins induce the expression of many target genes (Madhani *et al.* 1999; Roberts *et al.* 2000; Heise *et al.* 2010; Adhikari and Cullen 2014; van der Felden *et al.* 2014; Chow *et al.* 2019b; Zhou *et al.* 2020). Several highly induced targets of the fMAPK pathway positively regulate filamentous growth, such as *BUD8*, which encodes a protein involved in bud-site-selection at the distal pole [Figure 1A, (Zahner *et al.* 1996; Taheri *et al.* 2000; Ni and Snyder 2001; Cullen and Sprague 2002)]; *FLO11*, which encodes the major cell adhesion mucin-like flocculin [Figure 1A, (Lambrechts *et al.* 1996; Lo and Dranginis 1996, 1998; Madhani *et al.* 1999; Rupp *et al.* 1999; Guo *et al.* 2000; Cullen and Sprague 2012)]; and *CLN1*, which encodes a G_1 cyclin (Hadwiger *et al.* 1989), whose induction leads to a delay in the cell cycle resulting in an elongated cell morphology [Figure 1A, (Loeb *et al.* 1999; Madhani *et al.* 1999)]. Many other transcriptional targets remain uncharacterized, raising the possibility that the fMAPK pathway may have unappreciated roles in regulating filamentous growth.

A longstanding problem surrounding fMAPK pathway targets has been identifying phenotypes. One reason may be that some genes have a phenotype only noticeable under some conditions. Another reason is that targets might only contribute to a phenotype in a small way, if the cumulative effect of many genes is required to produce a phenotype. This means that some targets might have subtle phenotypes that could be overlooked. By examining cells lacking individual fMAPK pathway target genes under a variety of conditions for subtle but reproducible phenotypes, we identified new roles for five fMAPK pathway targets. One unexpected discovery that came from this approach was that the fMAPK pathway, which positively regulates invasive growth, can also negatively regulate aspects of invasive growth under some conditions. The other unexpected finding came from the characterization of a newly identified target, the transcription factor *SFG1* (Fujita *et al.* 2005; White *et al.* 2009), which enabled the fMAPK pathway to regulate cell adhesion and the cell cycle by multiple mechanisms. Our study suggests that these new functions for the fMAPK pathway provide an additional level of versatility, which presumably allows for more nuanced responses in different environments. Therefore, characterizing the targets of a signaling pathway can lead to new insights about how pathways regulate biological responses.

Materials and Methods

Yeast strains and plasmids

Yeast strains are listed in Table 1. Gene deletions were made through homologous recombination, constructed using auxotrophic or antibiotic resistance markers amplified by polymerase chain reaction (PCR) and introduced into yeast by lithium acetate transformation as described (Gietz 2014). Primers for PCR are listed in Supplemental Material, Table S1. Strains were verified by PCR southern analysis and phenotype, when possible. All strains are isogenic with HYL333 of the ∑1278b background [provided by G. Fink, Whitehead Institute for Biomedical Research, Cambridge, MA, (Liu *et al.* 1993)]. pRS316 plasmid is a control vector containing *URA3* as described in Sikorski and Hieter (1989) for experiments that use *ura*$^-$ strains. Yeast extract, peptone, dextrose (YPD) medium was used at the concentration of glucose specified (2%, 10%, 16%). For high osmolarity medium, sorbitol (sorb) is added to YPD medium (2% Glu + 8% Sorb). YP-GAL (2%), YPD medium except 2% galactose is used instead of dextrose. Synthetic complete medium (yeast nitrogen base without amino acids, dextrose (2%) or galactose (2%), amino acids) was also used. SD+AA, synthetic media with dextrose and amino acids; SD-URA, synthetic media with dextrose and amino acids minus uracil. SGAL-URA, synthetic medium with galactose and amino acids minus uracil. SLAD, synthetic low ammonium, dextrose (2%) (Gimeno *et al.* 1992).

Analysis of RNA sequencing data

RNA sequencing (RNAseq) analysis was previously performed in Adhikari and Cullen (2014). Here, the RNAseq data were visualized in a volcano plot generated using the program Instant Clue (http://www.instantclue.uni-koeln.de/). The plot was cropped to show targets induced by fMAPK (genes with a negative-fold change in the *ste12*Δ mutant).

Microscopy

For DIC (differential interference contrast) imaging, a Zeiss Axioplan 2 microscope (Oberkochen, Germany) was used. The digital images were acquired with an Axiocam MRm camera (Zeiss). For image acquisition and analysis, Axiovision 4.4 software (Zeiss) was used.

Plate-washing assay

The plate-washing assay was used to visualize differences in filamentous growth between the wild-type strain and mutants (Roberts and Fink 1994; Cullen 2015). Briefly, cells were spotted on medium as indicated at 30° for 1–10 days. Cells were spotted equidistant to each other and the edge of the plate to ensure uniform growth. Plates were placed under a stream of water, and colonies were rubbed gently by hand to remove noninvasive cells. Cells that remained in the agar after washing were considered to be part of the invasive scar. Images of the invasive scars were captured by ChemiDoc XRS+ molecular imager (from Bio-Rad Laboratories, Hercules, CA) under immunoblot/chemicoloric setting with no filter or a Nikon D3000 (Nikon, Garden City, NY) digital camera after the plate wash.

To quantify invasive growth, images from the plate-washing assay were imported into ImageJ (National Institutes of Health, Bethesda, MD; https://imagej.nih.gov/ij/). Each image was inverted and treated with identical parameters for adjusting brightness and contrast. For each image, the background was subtracted. Using the set threshold tool with light background set, a threshold was set to convert the invasive scars into pixel images. The threshold was set so that the area around the scar was excluded and areas of invasive growth were highlighted. The pixel area of each invasive scar was measured by the analyze particles tool. This was performed again for two additional higher thresholds (*i.e.*, 10, 30, and 50). The measured values from the three different threshold settings were totaled for a final value. Significance was determined for three replicates, separately for each type of media.

To quantify an invasive growth pattern, images of washed colonies were cropped to 350 × 350 pixels, inverted, and imported into ImageJ. Each image was treated with identical parameters for adjusting brightness and contrast. Images had their background subtracted with a value of 10,000 particles. A box was drawn across the midsection of the image with a pixel height of 40. Using the plot profile tool, which measures the gray value for pixels, a plot profile was generated for each strain of this region of the invasive scar and overlaid onto a graph in excel.

Measuring cell adhesion in liquid and from cells grown on semisolid agar media

To analyze cell adhesion in liquid media, cells were grown for 24 hr in YP-GAL (2%) media at 30°. Images were captured at 5× by microscopy and imported into ImageJ. The background was subtracted by 50 particles. A threshold was applied, set to 170, to convert the image into a binary pixel image. A scale of 1.266 μm per pixels was applied. Using the analyze particles tool, the area of cell clusters was measured and averaged. The averages of three replicates were used to calculate significance. Cells behaved the same if imaged directly in media or after being washed with water.

To analyze cell adhesion on semisolid media, cells were grown for 16 hr in SD+AA at 30°, washed in dH_2O, and cells were spotted onto YP-GAL (2%) medium. Plates were incubated at 30° for 3 days. Cells were harvested from colonies using a metal spatula with care not to excise the agar. Cell biomass was determined by weight. Cells were resuspended in 20 ml dH_2O in 50 ml conical tubes. Tubes were inverted vigorously by hand 10 times. The contents of the tube were poured into a Petri dish, and particles were photographed by ChemiDoc XRS+ molecular imager under immunoblot/chemicoloric setting with no filter. Images were imported into the GIMP2 program and cropped by 970 × 970 pixels circularly. The background was subtracted by 50.0 particles. A threshold was applied, set to 10, to generate a binary pixel image. Images were imported into ImageJ. A scale of 970 pixels = 82.13 mm based on measurements from the ChemiDoc XRS+ molecular imager and GIMP2 program (verified with ruler) was set. Using the analyze particles tool, the total area of cell adhesion was measured. Significance was determined for three replicates.

Colony immunoblots for Flo11p shedding

Colony immunoblots were performed as described (Karunanithi *et al.* 2010). Cells were grown in 3 ml SD+AA for 16 hr. Cells were pelleted and washed with dH_2O and spotted onto a nitrocellulose membrane directly on top of YP-GAL (2%) or YPD (2% Glu) plates. Plates were incubated at 30° for 3 days. Cells were washed off of the nitrocellulose by plate-washing. The nitrocellulose membrane was examined by immunoblot analysis with anti-HA antibodies and imaged by ChemiDoc XRS+ molecular imager. Signal intensity was measured with the volume tool in Image Lab (https://www.bio-rad.com/en-us/product/image-lab-software?ID=KRE6P5E8Z). Wild-type values were set to 1. Significance was determined for three replicates.

Biofilm/mat assays

Biofilm/mat assays were performed as described (Reynolds and Fink 2001; Karunanithi *et al.* 2012). Cells were grown in SD+AA for 16 hr and spotted onto semisolid agar (0.3%) medium for 3 days. To analyze plastic adhesion, cells were spotted onto YP-GAL (2%) plates and incubated at 30° for 3 days. Cells were then removed from the agar using a toothpick, resuspended in water, and adjusted to an optical density of A600 = 1.3. Aliquots (100 μl) of cell suspensions were added to polystyrene wells (96-well Falcon Microtest Tissue culture plate) and incubated for 4 hr. An equal volume of 1% crystal violet dye (DIFCO) was added to each well for 20 min. Wells were washed five times and photographed. Quantification was performed with ImageJ. Each well was circularly cropped 250 × 250 pixels from the center of the well. A threshold of 120 was set, then the analyze particle tool measured the total pixel area. Wild-type values were set to 1. Significance was determined for three replicates.

Comparative protein and gene sequence assessments

Comparative assessments for Nfg1p, Rgd2p, Rpi1p, Tip1p, and Sfg1p protein sequences were performed by BLAST (https://blast.ncbi.nlm.nih.gov/Blast.cgi). Nonredundant protein sequences (nr) was set for database. The algorithm was blastp (protein–protein BLAST). Sequences used were from the reference strain (S288c) downloaded from the *Saccharomyces* Genome Database (SGD) (https://www.yeastgenome.org/). Comparative assessment of synteny for *SFG1* was performed with the Yeast Gene Order Browser [(http://ygob.ucd.ie/), (Byrne and Wolfe 2005, 2006)].

Quantitative reverse transcription PCR

Quantitative reverse transcription PCR (RT-qPCR) was used to measure the relative expression of *FLO11* in wild type with pRS316 and the *nfg1*Δ, *rgd2*Δ, *rpi1*Δ, *tip1*Δ, *ste12*Δ, and *dig1*Δ mutants. Cells were spotted onto YPD (10% Glu) and incubated at 30° for 2 days. Cells were scraped from the surface of the agar, washed in 1 ml dH_2O, and harvested by centrifugation. RT-qPCR was also used to measure the relative expression of *FLO11*, *DSE1*, *DSE2*, *DSE4*, and *SCW11* in wild type and the *sfg1*Δ mutant. Cells were grown in 5 ml YPD (2% Glu) cultures grown at 30° for 23 hr. YPD (2% Glu) (1.5 ml) was pelleted and washed with 1 ml dH_2O; a 100 μl aliquot of washed cells was pipetted into 2 ml liquid YP-GAL (2%) cultures and incubated at 30° with shaking for 32 hr. After 32 hr, 2 ml of each sample was washed with 1 ml dH_2O and harvested by centrifugation. RT-qPCR was also used to verify targets of the fMAPK pathway by measuring the relative expression of *NFG1*, *RGD2*, *RPI1*, *TIP1*, and *SFG1* in wild type and the *ste12*Δ mutant. Cells were grown in 5 ml YPD (2% Glu) cultures grown at 30° for 16 hr; 1.5 ml of 16 hr cultures were pelleted and washed with 1 ml dH_2O. A 100 μl aliquot of washed cells was pipetted into YP-GAL (2%) liquid medium and incubated for 5.5 hr at 30°, washed with 1 ml dH_2O, and harvested by centrifugation. Cells not immediately used in RNA extractions were stored at −80°.

RNA was harvested by hot-acid phenol–chloroform extractions as described (Adhikari and Cullen 2014). Samples were further purified using a QIAGEN RNeasy Mini Kit (catalog number 74104; QIAGEN, Valencia, CA). RNA purity and concentration was measured with NanoDrop (NanoDrop 2000C; Thermo Fisher Scientific, Waltham, MA). RNA stability was determined by agarose gel electrophoresis. cDNA was generated and RT-qPCR was performed as previously described (Chow *et al.* 2019b). cDNA was generated using iScript Reverse Transcriptase Supermix (catalog number 1708841; Bio-Rad). RT-qPCR was performed using iTaq Universal SYBR Green Supermix (catalog number 1725121; Bio-Rad) on the Bio-Rad CFX384 Real Time System. Primers were obtained from Sigma (Sigma Chemical, St. Louis, MO). Primer sequences can be found in Table S2. *ACT1* housekeeping gene primers were based on Chow *et al.* (2019b). Primer sequences used for *FLO11* were based on Chen and Fink (2006). All starting gene concentrations were normalized to the housekeeping gene *ACT1* (Chavel *et al.* 2010; González *et al.* 2017). Relative gene expression was calculated using the $2-\Delta Ct$ formula; Ct was defined as the cycle where fluorescence was statistically significant above background (González *et al.* 2017); ΔCt is the difference in Ct between a target gene and the housekeeping gene (ACT1; González *et al.* 2017). RNA was prepared from three biological replicates. Average values are reported.

Measurement of fMAPK pathway activity

To analyze fMAPK pathway activity by the β-galactosidase (*lacZ*) assay, cells were grown in synthetic medium (SD-URA) for 16 hr. Cells were washed once in dH_2O and resuspended in the medium indicated for 4.5–6.5 hr of growth. Cells were harvested by centrifugation and stored at −80°. The *lacZ* assays were then performed as described (Jarvis *et al.* 1988; Cullen *et al.* 2000) using a *FUS1-lacZ* reporter as the readout of fMAPK pathway activity. To analyze fMAPK pathway activity by the *FUS1-HIS3* transcriptional (growth) reporter, strains were spotted onto SD-HIS+ATA (3-amino-1,2,4-triazole) medium and observed for growth after 3 days.

To analyze fMAPK pathway activity by phosphoblot analysis, cells were grown to saturation in SD-URA medium. Cells were washed and inoculated in 5 ml SD-URA for 5.5 hr at 30°. Cell extracts were prepared for immunoblot analysis according to established procedures (Lee and Dohlman 2008; Adhikari and Cullen 2014). Proteins were precipitated by trichloroacetic acid (TCA). Cells were lysed in TCA buffer (10 mM Tris-HCl pH 8.0; 10% TCA; 25 mM ammonium acetate; 1 mM EDTA) containing glass beads by vortexing for 1 min then placing on ice for 1 min five times. Cells were centrifuged at 15,000 × *g* for 10 min at 4° and the pellet was mixed in 150 μl of resuspension buffer (0.1 M Tris-HCl pH 11.0; 3% SDS) and boiled for 5 min at 95°. Samples were centrifuged at 15,000 × *g* for 5 min; 10 μl of each sample was used to measure protein concentration using Pierce BCA Protein Assay Kit (catalog# 23225; Thermo Scientific). An equal volume of 2× sodium dodecyl sulfate (SDS) loading dye (100 mM Tris-HCl pH 6.8; 4% SDS; 0.2% Bromophenol Blue; 20% glycerol; 200 mM β-mercaptoethanol) was added to the supernatant. Protein samples were separated on 10% SDS polyacrylamide gels (SDS-PAGE) and transferred to nitrocellulose membranes (Amersham Protran Premium 0.45 μm NC; GE Healthcare Life Sciences). The membrane was blocked in immunoblot buffer [5% nonfat dry milk (for Pgk1p and Kss1p) or 5% bovine serum albumin (BSA) (for P∼Kss1p), 10 mM Tris-HCl (pH 8), 150 mM NaCl, and 0.05% Tween 20] for 16 hr at 4° rocking. Radiance Plus Chemiluminescent substrate from Azure Biosystems (Dublin, CA) was used for detection. Mouse α-Pgk1p antibodies (#459250; Thermo Fisher Scientific, Rockford, IL) were used to detect Pgk1p as a loading control. Secondary antibodies, goat α-mouse

(#170-6516; Bio-Rad Laboratories), were used to detect primary antibodies (Pgk1p) for 1 hr at 20° with rocking. Phosphorylated Kss1p was detected by p42/p44 antibodies (#4370; Cell Signaling Technology, Danvers, MA) and total Kss1p was detected using α-Kss1p antibodies (#6775; Santa Cruz Biotechnology, Santa Cruz, CA). Secondary antibodies, goat anti-rabbit IgG-HRP (#111-035-144; Jackson ImmunoResearch Laboratories, West Grove, PA), were used to detect primary antibodies (Kss1p and P∼Kss1p) and incubated for 1 hr at 20° with rocking. The blot was imaged by ChemiDoc XRS+ molecular imager. Signal intensity was measured by using the volume tool in Image Lab (https://www.bio-rad.com/en-us/product/image-lab-software?ID=KRE6P5E8Z).

Data availability

The authors state that all data necessary for confirming the conclusions presented in the article are represented fully within the article. Strains and plasmids are available upon request. The Gene Expression Omnibus (GEO) accession number for the previously reported expression profiling data are GSE61783 (Adhikari and Cullen 2014). Supplemental material available at figshare: https://doi.org/10.25386/genetics.12609710.

Results

Characterizing transcriptional targets of the fMAPK pathway

Transcriptional targets of the fMAPK pathway have been identified by comparative expression profiling (Madhani *et al.* 1999; Roberts *et al.* 2000; Heise *et al.* 2010; Adhikari and Cullen 2014; van der Felden *et al.* 2014; Chow *et al.* 2019b). In Adhikari *et al.* (2014), wild-type cells and a fMAPK pathway mutant (*ste12*Δ) were compared in liquid YP-GAL (2% galactose) medium. YP-GAL (2%) medium is an fMAPK pathway-inducing condition that triggers the filamentous growth response (Karunanithi and Cullen 2012; Basu *et al.* 2020). The targets of the pathway identified in Adhikari *et al.* (2014) are shown here in a volcano plot cropped to display only induced targets (Figure 1B). Some highly induced genes are known targets of the pathway (Figure 1, A and B, blue circles, *FLO11* near the center of figure, *CLN1* right side of figure, *BUD8* right side of figure). Other well-characterized targets included *SUC2* (Figure 1B, blue circle near center of figure), which encodes the invertase responsible for hydrolyzing sucrose (Carlson *et al.* 1981) that contributes to social behaviors (Greig and Travisano 2004; Craig Maclean and Brandon 2008; Koschwanez *et al.* 2011) like the formation of invasive aggregates (Chow *et al.* 2019a); the fMAPK pathway components, *MSB2* [mucin sensor, (Cullen *et al.* 2004; Vadaie *et al.* 2008; Pitoniak *et al.* 2009)], *KSS1* [MAP kinase, (Courchesne *et al.* 1989; Roberts and Fink 1994; Bardwell *et al.* 1998a)], *STE12* and *TEC1* (Laloux *et al.* 1990; Chou *et al.* 2006) are induced by the fMAPK pathway to generate positive feedback (Figure 1, A and B, blue circles). *PGU1* encodes a pectinase (endopolygalacturonase) that does not affect filamentous growth but breaks down plant tissue and may impact nutrient scavenging in the wild (Madhani *et al.* 1999) (Figure 1B, black circle in center of figure). Several mating pathway targets were also identified that are under the control of Ste12p (Figure 1, *BAR1*, *STE2*, and *STE4*, black circles); however, the mating pathway is not thought to be required for filamentous growth (Roberts and Fink 1994; Sabbagh *et al.* 2001; Flatauer *et al.* 2005; Meem and Cullen 2012).

The fMAPK pathway also regulates the expression of targets whose functions remain uncharacterized. Thirteen new transcriptional targets were investigated (Figure 1B, green text, Figure S1) based on their fold change in expression as $\text{Log}_2\text{FoldChange} > |0.8|$. Gene disruptions were constructed in wild-type cells of the filamentous (Σ1278b) background, and deletion mutants were examined for a role in invasive growth. The plate-washing assay was used, where colonies washed off of a surface leave a visible invasive scar (Roberts and Fink 1994). We compared invasive scars of wild-type cells to mutants, looking for an invasive growth phenotype. Because invasive growth occurs in response to limiting carbon (Cullen and Sprague 2000, 2012) and nitrogen (Gimeno *et al.* 1992) and can be induced by high cell density through alcohols (Chen and Fink 2006; González *et al.* 2017; Lenhart *et al.* 2019), the plate-washing assay was performed on different media: YPD (2% Glu), YPD (10% Glu), YPD (16% Glu), YPD high osmolarity medium (2% Glu + 8% Sorbitol), SLAD (low nitrogen), SLAD + 2% ethanol, synthetic dextrose (SD), and YP-GAL (2%).

Most mutants tested did not show an obvious phenotype in invasive growth (Figure S1). Four mutants (*ylr042c*Δ, *rgd2*Δ, *rpi1*Δ, and *tip1*Δ, Figure 1B, yellow circles) did not show a phenotype on YPD (2% Glu), but showed increased invasive growth on YPD (10% Glu) (see below). This indicates unexpectedly that several highly induced targets of the fMAPK pathway function to negatively regulate invasive growth. Based on data shown below, *YLR042c* was named *NFG1* for Negative Regulator of the Filamentous Growth MAPK pathway 1. Among many mutants tested, one showed a clear invasive growth defect (*sfg1*Δ, Figure 1B, blue circle with green text, and Figure S1) and was also characterized in the study. Five target genes have paralogs that might mask their mutant phenotypes due to genetic redundancy or buffering (Wolfe and Shields 1997; Costanzo *et al.* 2010). Gene disruptions generating *prm5*Δ *ynl058c*Δ, *svs1*Δ *srl1*Δ, and *wsc2*Δ *wsc3*Δ double mutants did not show an invasive growth phenotype (Figure S1). Gene disruptions for *RIB4*, *SRD1*, *HPF1*, *ADA2*, *AAD3* (paralog to *AAD15*), and *PRY1* (paralog to *PRY2*) failed to obtain positive isolates. A genome-wide deletion collection in the Σ1278b background did not contain deletion mutants of *SRD1*, *AAD3*, *RIB4*, *HPF1*, and *AAD15* (Ryan *et al.* 2012), but did for *ADA2*, *PRY1*, and *PRY2*, which did not show an invasive growth phenotype (Ryan *et al.* 2012; Chavel *et al.* 2014). We were successful at assigning roles based on

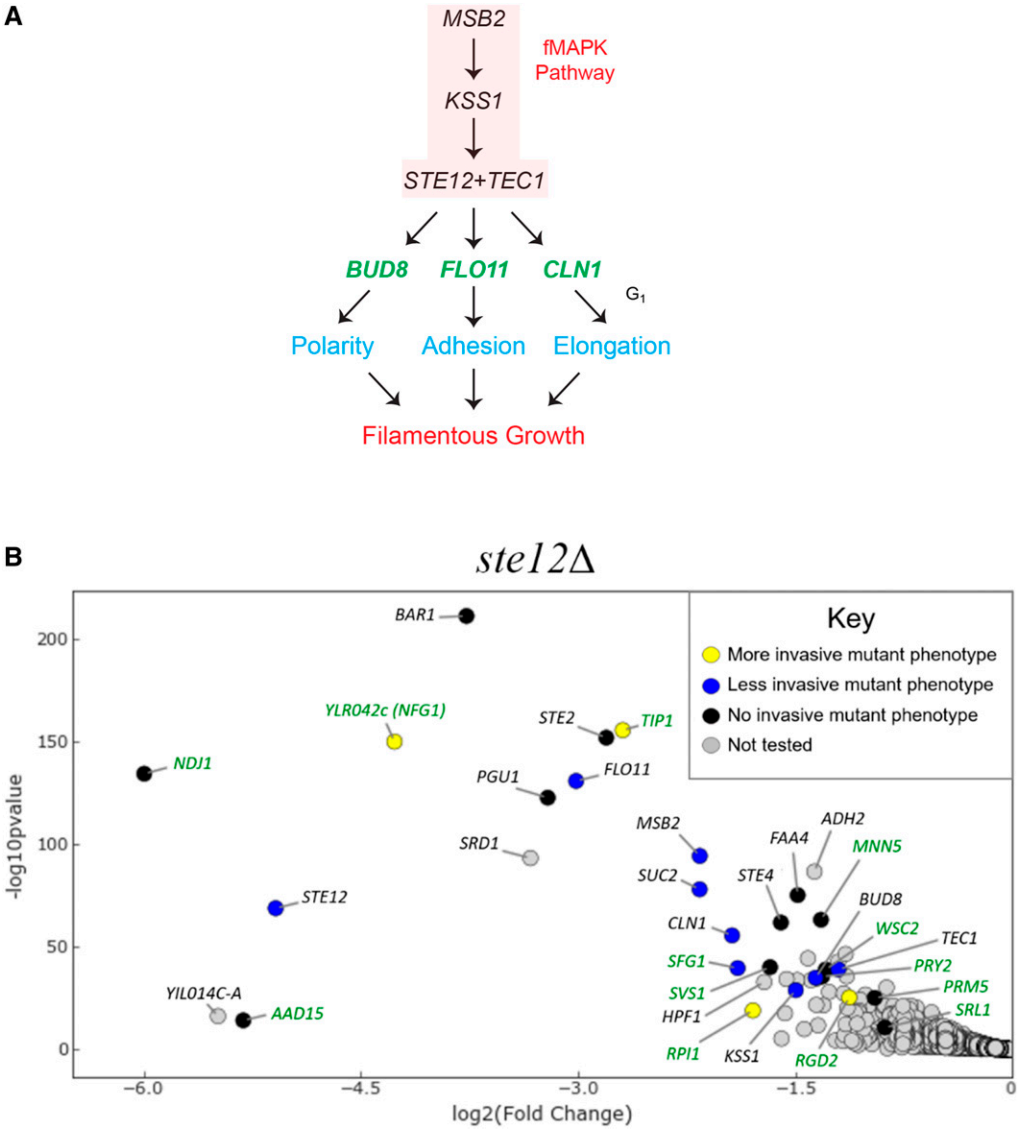

Figure 1 Phenotypic analysis for invasive growth of transcriptional targets of the fMAPK pathway identified by comparative RNAseq analysis. (A) A model for the MAPK pathway that regulates filamentous growth by inducing target genes (green) that promote cell adhesion (*FLO11*), cell elongation at G_1 (*CLN1*), and distal-pole budding (*BUD8*). Pathway components are highlighted in red (*MSB2*, *KSS1*, *STE12*, *TEC1*). Not all pathway components are shown. (B) Portion of a volcano plot showing RNAseq data from a previous study (Adhikari and Cullen 2014). *x*-axis, $\log_2$(FC); *y*-axis, $-\log_{10}$(*P*-value). Fold change in gene expression between *ste12*Δ and wild-type cells grown in YP-Gal (2%) for 5.5 hr. All genes labeled have $|\log_2(\text{FC})| > 0.85$ and *P*-value $< 2.5 \times 10^{-11}$. Transposable elements and dubious open reading frames not shown in the graph. Green text, genes tested in the study. Yellow, more invasive mutant phenotype. Blue, less invasive mutant phenotype. Black, no invasive mutant phenotype. Gray, not tested.

phenotype to 5 of 13 (38%) of the target genes tested. However, 62% of the genes failed to produce a phenotype. It is plausible that these genes function in aspects of filamentous growth that are unrelated to agar invasion [for example, Pgu1p (Madhani *et al.* 1999)]. Genes that showed a phenotype in invasive growth were verified as targets of the fMAPK pathway by examining their expression by RT-qPCR analysis under conditions that promote filamentous growth (Figure S2, YP-GAL medium). *NFG1*, *RGD2*, *RPI1*, *TIP1*, and *SFG1* may be direct targets because the transcription factors Ste12p and Tec1p bind to their promoters based on the repository YEASTRACT [http://www.yeastract.com/index.php, (Zeitlinger *et al.* 2003; Harbison *et al.* 2004; Borneman *et al.* 2007; Lefrançois *et al.* 2009; Zheng *et al.* 2010)]. Thus, four negative regulators of invasive growth (*NFG1*, *RGD2*, *RPI1*, and *TIP1*) and one positive regulator of invasive growth (*SFG1*) were identified here as fMAPK pathway targets.

The fMAPK pathway induces target genes that negatively regulate invasive growth

A major function of the fMAPK pathway is to positively regulate invasive growth [Figure S1, *ste12*Δ (Roberts and Fink 1994; Cook *et al.* 1997; Roberts *et al.* 2000)]. On YPD (10% Glu) medium, the *nfg1*Δ, *rgd2*Δ, *rpi1*Δ, and *tip1*Δ mutants showed increased invasive growth compared to wild type (Figure 2A, Washed), which was confirmed by quantification by ImageJ (Figure 2A, Invasion). Thus, Nfg1p, Rgd2p, Rpi1p, and Tip1p have a negative effect on invasive growth. *NFG1* is a highly induced ORF by the fMAPK pathway that has been established as a target for some time with no described function in invasive growth [*YLR042c*, (Caro *et al.* 1997; Hamada *et al.* 1999; Madhani *et al.* 1999; Roberts *et al.* 2000; Giaever *et al.* 2002; Hohmann 2002; García *et al.* 2004; Kim and Levin 2010; Parachin *et al.* 2010; Adhikari and Cullen 2014; Chow *et al.* 2019b)]. *TIP1* encodes a

Table 1 Yeast strains used in this study

Strain	Description	Reference
PC538	*MAT***a** *SY3089 ste4 FUS1-lacZ FUS1-HIS3 ura3-52*	Cullen *et al.* (2004)
PC539	*MAT***a** *SY3089 ste4 FUS1-lacZ FUS1-HIS3 ura3-52 ste12::URA3*	Pitoniak *et al.* (2009)
PC611	*MAT***a** *SY3089 ste4 FUS1-lacZ FUS1-HIS3 ura3-52 ste11::URA3*	Cullen and Sprague (2002)
PC1029	*MAT***a** *SY3089 ste4 FUS1-lacZ FUS1-HIS3 ura3-52 flo11::KanMX6*	Karunanithi *et al.* (2010)
PC2043	*MAT***a** *SY3089 ste4 FUS1-lacZ FUS1-HIS3 ura3-52 FLO11-HA at 1000aa*	Karunanithi *et al.* (2010)
PC2712	*MAT***a** *SY3089 ste4 FUS1-lacZ FUS1-HIS3 ura3-52 GAL-FLO11*	Karunanithi *et al.* (2010)
PC3039	*MAT***a** *SY3089 ste4 FUS1-lacZ FUS1-HIS3 ura3-52 Msb2-HA at 500aa dig1::KlURA3*	Chavel *et al.* (2010)
PC7144	*MAT***a** *SY3089 ste4 FUS1-lacZ FUS1-HIS3 ura3-52 sfg1::KlURA3*	This study
PC7145	*MAT***a** *SY3089 ste4 FUS1-lacZ FUS1-HIS3 ura3-52 rpi1::KlURA3*	This study
PC7146	*MAT***a** *SY3089 ste4 FUS1-lacZ FUS1-HIS3 ura3-52 rgd2::KlURA3*	This study
PC7147	*MAT***a** *SY3089 ste4 FUS1-lacZ FUS1-HIS3 ura3-52 nfg1::KlURA3*	This study
PC7164	*MAT***a** *SY3089 ste4 FUS1-lacZ FUS1-HIS3 ura3-52 dse1::KlURA3*	This study
PC7165	*MAT***a** *SY3089 ste4 FUS1-lacZ FUS1-HIS3 ura3-52 dse2::KlURA3*	This study
PC7166	*MAT***a** *SY3089 ste4 FUS1-lacZ FUS1-HIS3 ura3-52 dse4::KlURA3*	This study
PC7167	*MAT***a** *SY3089 ste4 FUS1-lacZ FUS1-HIS3 ura3-52 svs1::KlURA3*	This study
PC7168	*MAT***a** *SY3089 ste4 FUS1-lacZ FUS1-HIS3 ura3-52 ndj1::KlURA3*	This study
PC7169	*MAT***a** *SY3089 ste4 FUS1-lacZ FUS1-HIS3 ura3-52 prm5::KlURA3*	This study
PC7170	*MAT***a** *SY3089 ste4 FUS1-lacZ FUS1-HIS3 ura3-52 wsc2::KlURA3*	This study
PC7198	*MAT***a** *SY3089 ste4 FUS1-lacZ FUS1-HIS3 ura3-52 scw11::KlURA3*	This study
PC7200	*MAT***a** *SY3089 ste4 FUS1-lacZ FUS1-HIS3 ura3-52 wsc3::NAT*	This study
PC7201	*MAT***a** *SY3089 ste4 FUS1-lacZ FUS1-HIS3 ura3-52 ynl058c::NAT*	This study
PC7202	*MAT***a** *SY3089 ste4 FUS1-lacZ FUS1-HIS3 ura3-52 svs1::KlURA3 srl1::NAT*	This study
PC7203	*MAT***a** *SY3089 ste4 FUS1-lacZ FUS1-HIS3 ura3-52 prm5::KlURA3 ynl058c::NAT*	This study
PC7238	*MAT***a** *SY3089 ste4 FUS1-lacZ FUS1-HIS3 ura3-52 aad15::KlURA3*	This study
PC7239	*MAT***a** *SY3089 ste4 FUS1-lacZ FUS1-HIS3 ura3-52 hug1::KlURA3*	This study
PC7240	*MAT***a** *SY3089 ste4 FUS1-lacZ FUS1-HIS3 ura3-52 pyr2::KlURA3*	This study
PC7241	*MAT***a** *SY3089 ste4 FUS1-lacZ FUS1-HIS3 ura3-52 mnn5::KlURA3*	This study
PC7243	*MAT***a** *SY3089 ste4 FUS1-lacZ FUS1-HIS3 ura3-52 wsc2::KlURA3 wsc3::NAT*	This study
PC7277	*MAT***a** *SY3089 ste4 FUS1-lacZ FUS1-HIS3 ura3-52 tip1::KlURA3*	This study
PC7280	*MAT***a** *SY3089 ste4 FUS1-lacZ FUS1-HIS3 ura3-52 flo11::Km sfg1::-KlURA3*	This study
PC7281	*MAT***a** *SY3089 ste4 FUS1-lacZ FUS1-HIS3 ura3-52 GAL-FLO11 sfg1::KlURA3*	This study
PC7306	*MAT***a** *SY3089 ste4 FUS1-lacZ FUS1-HIS3 ura3-52 rho5::NAT*	This study
PC7321	*MAT***a** *SY3089 ste4 FUS1-lacZ FUS1-HIS3 ura3-52 FLO11-HA at 1000aa sfg1::KlURA3*	This study
PC7536	*MAT***a** *SY3089 ste4 FUS1-lacZ FUS1-HIS3 ura3-52 nfg1::KlURA3 tip1::NAT*	This study
PC7556	*MAT***a** *SY3089 ste4 FUS1-lacZ FUS1-HIS3 ura3-52 nfg1::KlURA3 tip1::NAT rgd2::KanMX6*	This study
PC7557	*MAT***a** *SY3089 ste4 FUS1-lacZ FUS1-HIS3 ura3-52 nfg1::KlURA3 tip1::NAT rgd2::KanMX6 rpi1::HYG*	This study

mannoprotein of the fungal cell wall (Kondo and Inouye 1991; Fujii *et al.* 1999; Chow *et al.* 2018) and *RGD2* encodes a GTPase-activating protein (RhoGAP for Cdc42p and Rho5p; Roumanie *et al.* 2001; Tkach *et al.* 2012), both with no established role in invasive growth. *RPI1* encodes a transcription factor that inhibits the Ras/cyclic AMP pathway (Kim and Powers 1991), promotes preparation of cells for the stationary phase in part by fortification of the cell wall (Sobering *et al.* 2002), and increases stress tolerance during fermentation (Puria *et al.* 2009). *RPI1* was previously shown to promote filamentous growth in some strain backgrounds but not in the ∑1278b strain background (Chin *et al.* 2012).

When compared to the *dig1*Δ mutant, which lacks a known negative regulator of the fMAPK pathway (Cook *et al.* 1996; Tedford *et al.* 1997; Bardwell *et al.* 1998b; Olson *et al.* 2000), the *nfg1*Δ, *rgd2*Δ, *rpi1*Δ, and *tip1*Δ mutants had more subtle phenotypes (Figure 2A). This suggests Nfg1p, Rgd2p, Rpi1p, and Tip1p might not turn off invasive growth like Dig1p, but instead modulate it in a specific context. One way the fMAPK pathway regulates invasive growth is by regulating the expression of *FLO11*, which encodes the cells' major adhesion molecule (Lo and Dranginis 1996; Madhani *et al.* 1999; Rupp *et al.* 1999; Roberts *et al.* 2000; Halme *et al.* 2004; Borneman *et al.* 2006; Veelders *et al.* 2010; Adhikari and Cullen 2014;

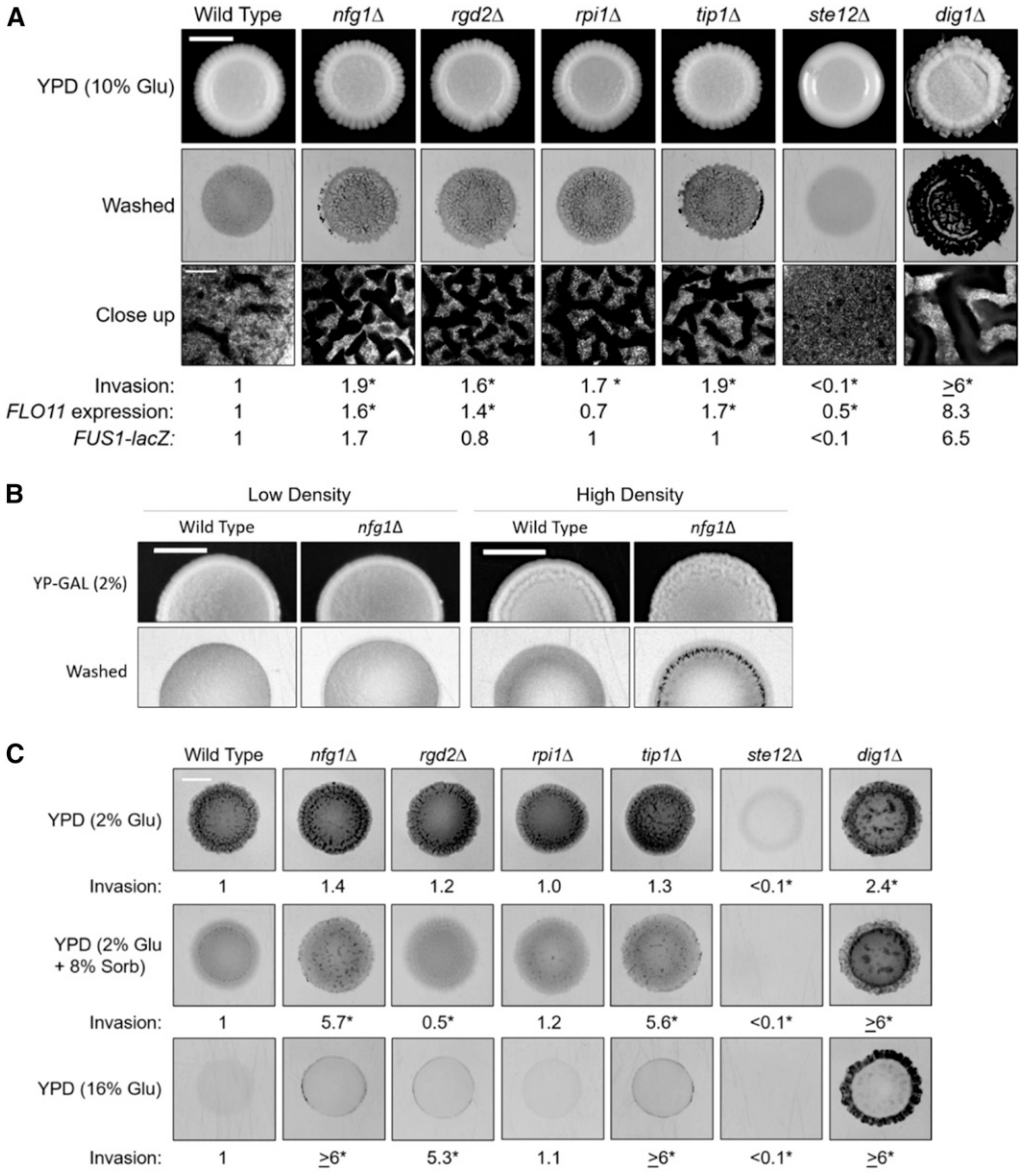

Figure 2 Four targets of the fMAPK pathway negatively regulate invasive growth. (A) Plate-washing assay. Wild-type cells (PC538+pRS316) and the *nfg1*Δ (PC7147), *rgd2*Δ (PC7146), *rpi1*Δ (PC7145), *tip1*Δ (PC7277), *ste12*Δ (PC539), and *dig1*Δ (PC3039) mutants were spotted on YPD (10% Glu) for 3 days. Top row, colonies, middle row, inverted images of plates after wash, Bar, 0.5 cm. Bottom row, close-up of washed plates showing aggregates at 5× magnification, Bar, 400 μm. Invasion, quantification of invasive scars by ImageJ in triplicate, with wild-type values set to 1. Error represents the SEM, which varied <20% across trials. Asterisks, *P*-value <0.035, by Student's *t*-test compared to wild type. *FLO11* expression, fold change in *FLO11* mRNA levels by RT-qPCR analysis normalized to *ACT1*. Wild-type values were set to 1. Variance by SD. was <20% across three trials for all strains, except the *dig1*Δ mutant, which was one trial. Asterisks, *P*-value ≤0.01, by Student's *t*-test compared to wild type. *FUS1-lacZ*, β-Galactosidase (*lacZ*) assays. Cells were grown in SD-URA for 16 hr, washed, and resuspended in SGAL-URA for 4.5 hr prior to harvesting cells by centrifugation. (B) Plate-washing assay for wild-type cells (PC538+pRS316) and the *nfg1*Δ mutant (PC7147) grown on YP-Gal (2%) medium. Top row, colonies, bottom row, inverted images of plates after wash, Bar, 0.5 cm. Low Density, cells spotted with OD_{600} = 1.5 for 3 d. High Density, cells spotted with OD_{600} = 11 for 2 days. (C) Plate-washing assay on YPD (2% Glu), high osmolarity medium [YPD (2% Glu + 8% Sorb)], and YPD (16% Glu) for 3 day. Inverted images of plates after wash for indicated strains, Bar, 0.5 cm. Colonies (not shown) were similar in size and appearance. Invasion, quantification of invasive scars by ImageJ in triplicate, with wild type values set to 1. Error represents the SEM, which varied <30% across trials, except the *rpi1*Δ mutant on YPD (16% Glu) varied by <75%. Asterisks, *P*-value < 0.05, by Student's *t*-test compared to wild type. (D) Immunoblot analysis of wild type cells (PC538+pRS316) and the *nfg1*Δ (PC7147) and *ste11*Δ (PC611) mutants grown in SD-URA for 5.5 hr. Cell extracts were probed with antibodies to detect phosphorylated Kss1p (P∼Kss1p) [α-p42/p44], total Kss1p, and Pgk1p as a control for protein levels. Numbers refer to the ratio of P∼Kss1p to Pgk1p with wild type set to 1. The MAP kinase for the mating pathway, Fus3p, also showed some elevated phosphorylation, as might be expected based on a previous report (Basu *et al.* 2016).

Kraushaar *et al.* 2015; Barua *et al.* 2016; Reynolds 2018; Chow *et al.* 2019b; Brückner *et al.* 2020). RT-qPCR analysis showed that the expression of *FLO11* was elevated in the *nfg1*Δ, *rgd2*Δ, and *tip1*Δ mutants compared to wild type, indicating these genes have an inhibitory effect on *FLO11* expression (Figure 2A, *FLO11* expression). The effect was modest (∼0.5-fold), which supports the idea that these genes may be involved in fine tuning invasive growth. As in previous findings (Chin *et al.* 2012), the *rpi1*Δ mutant showed no change in the expression of *FLO11* compared to wild type (Figure 2A, *FLO11* expression).

Closer inspection of the invasive scars showed an increase in aggregate invasive growth (Figure 2A, Close up), which results from the interaction of groups of cells that make gouges in the agar (Chow *et al.* 2019a). Likewise, the *nfg1*Δ, *rgd2*Δ, *rpi1*Δ, and *tip1*Δ mutants showed elevated aggregate invasive growth on YP-GAL (2%) medium; however, this occurred only when cells were spotted at high cell density (Figure 2B, the complete data set is in Figure S3), which stimulates aggregate invasive growth due to an increased abundance of quorum-sensing molecules (Chow *et al.* 2019a). At standard glucose concentrations [YPD (2% Glu) medium], the *rgd2*Δ, *rpi1*Δ, and *tip1*Δ mutants were not more invasive than wild type, and *nfg1*Δ was only slightly more invasive at a *P*-value < 0.062 [Figure 2C, YPD (2% Glu)]. These results indicate Nfg1p, Rgd2p, Rpi1p, and Tip1p inhibit invasive growth more noticeably at higher glucose levels. This observation was puzzling because glucose inhibits invasive growth (Cullen and Sprague 2000). One possibility is that high glucose levels might lead to higher cell density as a result of an elevated carrying capacity (Spor *et al.* 2008). High carrying capacity may lead to enhanced density-dependent invasion after depletion of glucose. Thus, the Nfg1p, Rgd2p, Rpi1p, and Tip1p proteins negatively regulate aggregate invasive growth.

Nfg1p, Rgd2p, Rpi1p, and Tip1p might act separately or in the same pathway. To address this question, the *nfg1*Δ, *rgd2*Δ, *rpi1*Δ, and *tip1*Δ mutants were compared by different assays and in different conditions to see if they share the same phenotype. Sharing the same phenotype would suggest that the proteins act in the same pathway. The *nfg1*Δ and *tip1*Δ mutants were phenotypically similar, showing increased invasive growth on different types of media: YPD (10% Glu) [Figure 2A, invasion], YP-GAL (2%) (Figure S3B), high osmolarity medium [YPD (2% Glu + 8% Sorb), Figure 2C], and YPD (16% Glu) (Figure 2C). The *nfg1*Δ and *tip1*Δ mutants also showed the same pattern of *FLO11* expression (Figure 2A, *FLO11* expression). These results support the idea that Nfg1p and Tip1p act in the same pathway.

The *rgd2*Δ and *rpi1*Δ mutants were phenotypically similar to the *nfg1*Δ and *tip1*Δ mutants on some media, showing increased invasive growth on YPD (10% Glu) [Figure 2A, invasion] and YP-GAL (2%) (Figure S3B). However, the *rgd2*Δ and *rpi1*Δ mutants were phenotypically different from the *nfg1*Δ and *tip1*Δ mutants because they did not show increased invasive growth on high osmolarity medium [YPD (2% Glu + 8% Sorb), Figure 2C]. The *rgd2*Δ and *rpi1*Δ mutants were also phenotypically different from each other on high osmolarity medium [YPD (2% Glu + 8% Sorb), Figure 2C] and YPD (16% Glu) (Figure 2C). Furthermore, Rgd2p but not Rpi1p regulated *FLO11* expression (Figure 2A, *FLO11* expression). Overall, these results suggest Rgd2p and Rpi1p function in different pathways.

Mutant combinations were generated (*nfg1*Δ *tip1*Δ double mutant, *nfg1*Δ *tip1*Δ *rgd2*Δ triple mutant, and *nfg1*Δ *tip1*Δ *rgd2*Δ *rpi1*Δ quadruple mutant) to determine if they had additive phenotypes. Additive phenotypes would suggest the proteins operate in different pathways. The *nfg1*Δ single mutant, the *nfg1*Δ *tip1*Δ double mutant, the *nfg1*Δ *tip1*Δ *rgd2*Δ triple mutant, and the *nfg1*Δ *tip1*Δ *rgd2*Δ *rpi1*Δ quadruple mutant showed increased invasive growth compared to wild type but did not show strong phenotypic differences from each other by the plate-washing assay (Figure S4, A and B). Collectively, evidence from the plate-washing assay of single mutants and mutant combinations suggests Rgd2p and Rpi1p function separately from each other and from Nfg1p and Tip1p, while Nfg1p and Tip1p may act in the same pathway.

The fMAPK pathway is one of the pathways that regulates *FLO11* expression (Madhani *et al.* 1999; Rupp *et al.* 1999; Borneman *et al.* 2006; Chavel *et al.* 2010, 2014; Cullen and Sprague 2012). Given that Nfg1p, Rgd2p, and Tip1p have a negative effect on *FLO11* expression, they might do so by dampening the fMAPK pathway. The *nfg1*Δ mutant, but not the *tip1*Δ, *rgd2*Δ, or *rpi1*Δ mutant showed elevated fMAPK pathway activity based on a transcriptional reporter [Figure 2A, *FUS1-lacZ*]. This indicates that Nfg1p negatively regulates the fMAPK pathway. Double, triple, and quadruple mutant analysis showed that the *nfg1*Δ *tip1*Δ double mutant had an additional increase in fMAPK pathway activity compared to the *nfg1*Δ single mutant (Figure S4A, *FUS1-lacZ*). Thus, Tip1p might also negatively regulate the fMAPK pathway under some conditions separately from Nfg1p, although we have not explored this possibility. These results indicate Nfg1p and Tip1p act, at least in part, in separate ways. Immunoblot analysis with antibodies that detect phosphorylated (P∼) Kss1p (the MAP Kinase of the fMAPK pathway) showed that P∼Kss1p levels were higher in the *nfg1*Δ mutant (Figure 2D), compared to wild-type cells and the *ste11*Δ mutant [Ste11p is the MAP kinase kinase kinase that phosphorylates the MAP kinase kinase, Ste7p, which phosphorylates Kss1p (Liu *et al.* 1993; Roberts and Fink 1994)]. Thus, Nfg1p, Rgd2p, Rpi1p, and Tip1p have separate functions in the negative regulation of invasive growth, and Nfg1p (and perhaps Tip1p) negatively regulates the fMAPK pathway.

We performed comparative assessments of Nfg1p, Rgd2p, Rpi1p, and Tip1p by BLAST. Nfg1p protein sequence had similarity only within the *Saccharomyces* clade, with *Saccharomyces eubayanus* being the most distant relative with a recognizable homolog (Figure S5, A and B); therefore, Nfg1p is not a conserved protein that regulates the fMAPK pathway across all yeasts. The protein sequences of Rgd2p,

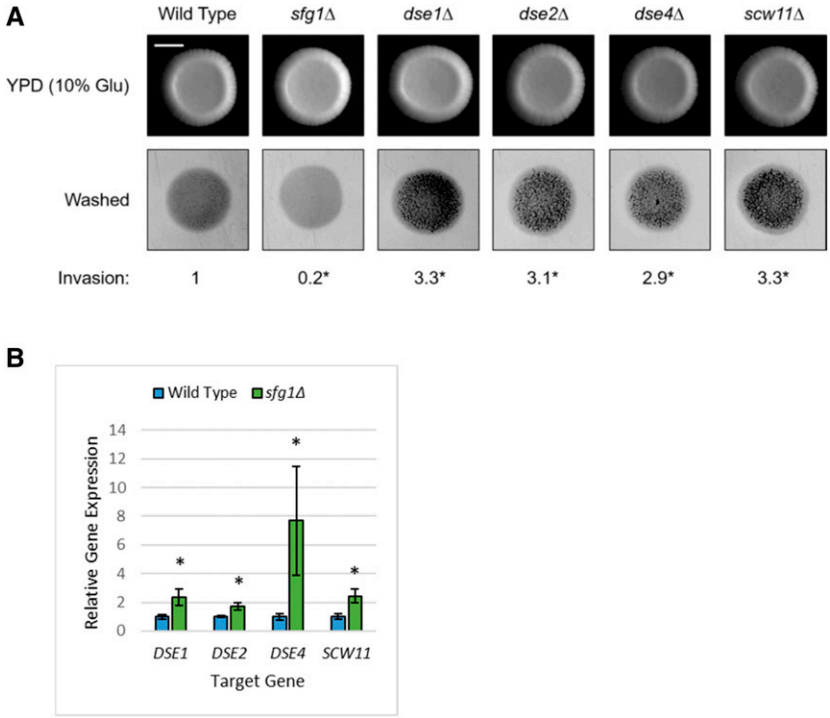

Figure 3 Transcriptional targets of Sfg1p that induce cell separation inhibit invasive growth. (A) Plate-washing assay for wild-type cells (PC538+pRS316) and the *sfg1*Δ (PC7144), *dse1*Δ (PC7164), *dse2*Δ (PC7165), *dse4*Δ (PC7166), and *scw11*Δ (PC7198) mutants spotted onto YPD (10% Glu) for 3 days. Top row, colonies, bottom row, inverted images of invasive scar after plate wash, Bar, 0.5 cm. Invasion, quantification of invasive scars by ImageJ in triplicate, with wild-type values set to 1. Error represents the SEM, which varied <45% across trials, except the *sfg1*Δ mutant which varied by <56%. Asterisks, *P*-value <0.035, by Student's *t*-test compared to wild type. (B) Relative gene expression by RT-qPCR of target gene (*DSE1*, *DSE2*, *DSE4*, and *SCW11*) mRNA levels, normalized to *ACT1* expression, between wild-type (PC538) and *sfg1*Δ (PC7144) cells grown in YP-Gal (2%) liquid medium for 32 hr. Wild-type values set to 1. Error represents SD across three trials. Asterisks, *P*-value < 0.02, by Student's *t*-test compared to wild type.

Rpi1p, and Tip1p had homologs in other yeasts outside the *Saccharomyces* clade (Figure S5, A and B), including *Candida glabrata*—a human pathogen that undergoes filamentous growth (Fidel *et al.* 1999; Csank and Haynes 2000; Rodrigues *et al.* 2014). Rgd2p also had protein sequence similarity to a homolog in the human pathogen *C. albicans* (Figure S5, A and B). Thus, Rgd2p, Rpi1p, and Tip1p are conserved in several yeast species and could be regulators of filamentous growth in pathogenic yeasts.

Sfg1p negatively regulates the transcription of cell separation genes

SFG1 was identified as a target of the fMAPK pathway (Figure 1B, blue circle with green text) and positive regulator of invasive growth (Figure S1, Third column). Sfg1p is a transcription factor that induces superficial pseudohyphal growth [a type of growth where cells spread across a surface in filament-like structures (Fujita *et al.* 2005)] and transcriptionally represses genes that induce cell separation, including *DSE1*, *DSE2*, *DSE4*, and *SCW11* (Doolin *et al.* 2001; Baladrón *et al.* 2002; Draper *et al.* 2009; White *et al.* 2009). The inhibition of cell separation leads to filament formation (King and Butler 1998; Doolin *et al.* 2001). *DSE2*, *DSE4*, and *SCW11* have similarity to glucanases and may promote cell separation by degrading the cell wall between mother and daughter cells. To determine whether Sfg1p regulates invasive growth by this mechanism, the transcriptional targets of Sfg1p that induce cell separation were tested for a role in invasive growth. Wild-type cells and the *sfg1*Δ, *dse1*Δ, *dse2*Δ, *dse4*Δ and *scw11*Δ mutants were examined for invasive growth by the plate-washing assay (Figure 3A). The *dse1*Δ, *dse2*Δ, *dse4*Δ and *scw11*Δ mutants had increased invasive growth compared to wild-type cells, supporting the idea that these genes have an inhibitory effect on invasive growth. *DSE1*, *DSE2*, *DSE4* and *SCW11* were transcriptional targets of Sfg1p by RT-qPCR analysis being upregulated in the *sfg1*Δ mutant under conditions that promote filamentous growth (Figure 3B, YP-GAL medium). Thus, in support of previous findings, Sfg1p inhibits the transcription of genes that promote cell separation, which results in increased cell attachment and invasive growth.

SFG1 regulates invasive growth independently from FLO11

One requirement for invasive growth is cell adhesion by Flo11p (Lo and Dranginis 1996; Madhani *et al.* 1999; Rupp *et al.* 1999; Halme *et al.* 2004; Borneman *et al.* 2006; Veelders *et al.* 2010; Kraushaar *et al.* 2015; Barua *et al.* 2016; Reynolds 2018). Flo11p binds in a homotypic manner to other Flo11p molecules to maintain adhesive contacts between cells (Kraushaar *et al.* 2015; Brückner *et al.* 2020). The expression of *FLO11* is regulated by the fMAPK pathway (Madhani *et al.* 1999; Rupp *et al.* 1999; Roberts *et al.* 2000; Borneman *et al.* 2006; Adhikari and Cullen 2014; Chow *et al.* 2019b). Presumably, Sfg1p (by inhibiting cell separation) and Flo11p (by promoting homotypic contacts) function in different ways to control filamentous growth. The fact that *SFG1* and *FLO11* expression are both regulated by the fMAPK pathway suggests that the pathway may have versatility in regulating cell adhesion through a combination of mechanisms.

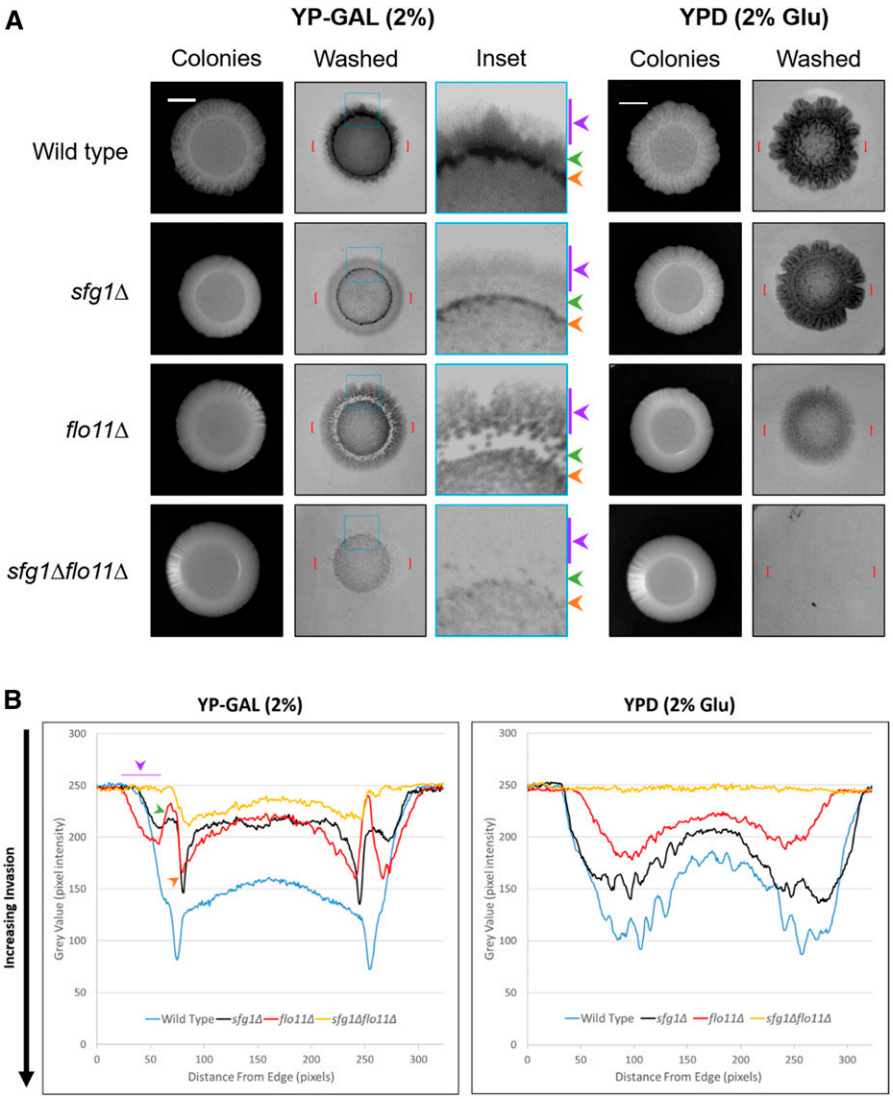

Figure 4 Sfg1p is required for invasive growth and has a different phenotype than Flo11p. (A) Plate-washing assay for wild type (PC538), *sfg1*Δ (PC7144), *flo11*Δ (PC1029), and *sfg1*Δ*flo11*Δ (PC7280) strains spotted on YP-Gal (2%) medium and YPD (2% Glu) medium for 7 days. Left columns, colonies, Washed, inverted images of invasive scar after plate wash, Bar, 0.5 cm. Inset, close up of invasive scars on YP-GAL (2%) marked on washed images by blue box. Orange arrows, ring region of invasive scar. Green arrows, region directly outside invasive ring. Purple arrows, periphery of invasive scar. (B) Plot of invasion across each invasive scar from (A) (Washed, red brackets represent outside edge of region used for measurement). *X*-axis, distance in pixels from left edge; *Y*-axis, intensity of invasion measured by gray area intensity of pixels in ImageJ. High values, less invasive growth, low values more invasive growth. Colored arrows mark regions denoted in (A).

To explore how Sfg1p and Flo11p regulate cell adhesion and invasive growth, a double gene deletion mutant was generated (*sfg1*Δ *flo11*Δ). Wild-type cells were compared to the *sfg1*Δ and *flo11*Δ single mutants and the *sfg1*Δ *flo11*Δ double mutant by the plate-washing assay. On YP-GAL (2%) medium, the *sfg1*Δ and *flo11*Δ single mutants showed a defect in invasive growth [Figure 4A, YP-GAL (2%), the complete data set is in Figure S6A]. The *sfg1*Δ *flo11*Δ double mutant had a more severe invasive growth defect than either single mutant [Figure 4A, YP-GAL (2%)]. These data demonstrate that Sfg1p and Flo11p play separate roles in regulating invasive growth. Moreover, the *sfg1*Δ *flo11*Δ double mutant retained some invasive growth, which indicates that a third (*FLO11*- and *SFG1*-independent) mechanism also regulates invasive growth under this condition. Flo11p is a member of the Flo gene family (Guo *et al.* 2000; Smukalla *et al.* 2008; Veelders *et al.* 2010), and, although other members of this family are typically silenced, another Flo gene may be expressed under this condition. *FLO10* is expressed at least to some degree in our strains (Birkaya *et al.* 2009; Chow *et al.* 2018) and may contribute to invasive growth in this setting.

The *sfg1*Δ and *flo11*Δ single mutants had different invasive patterns. To better visualize the patterns, invasive scars were quantified by ImageJ and represented graphically by a plot profile. ImageJ was used to measure pixel intensity across the invasive scar (Figure 4A, Washed, see red brackets), with higher values (lighter pixels) representing less invasion and lower values (darker pixels) representing more invasion. For wild-type cells, invasive growth occurred in a unique pattern, with the most intense invasive growth occurring as a ring (Figure 4A, Inset, orange arrow), which corresponded to two troughs in the graph [Figure 4B, YP-Gal (2%), blue line]. The *sfg1*Δ mutant was less invasive than wild-type cells but still produced an invasive ring [Figure 4B, YP-Gal (2%), black line]. The *sfg1*Δ mutant showed a similar level of invasion as the *flo11*Δ mutant [Figure 4B, YP-Gal (2%), compare black and red lines] but was more

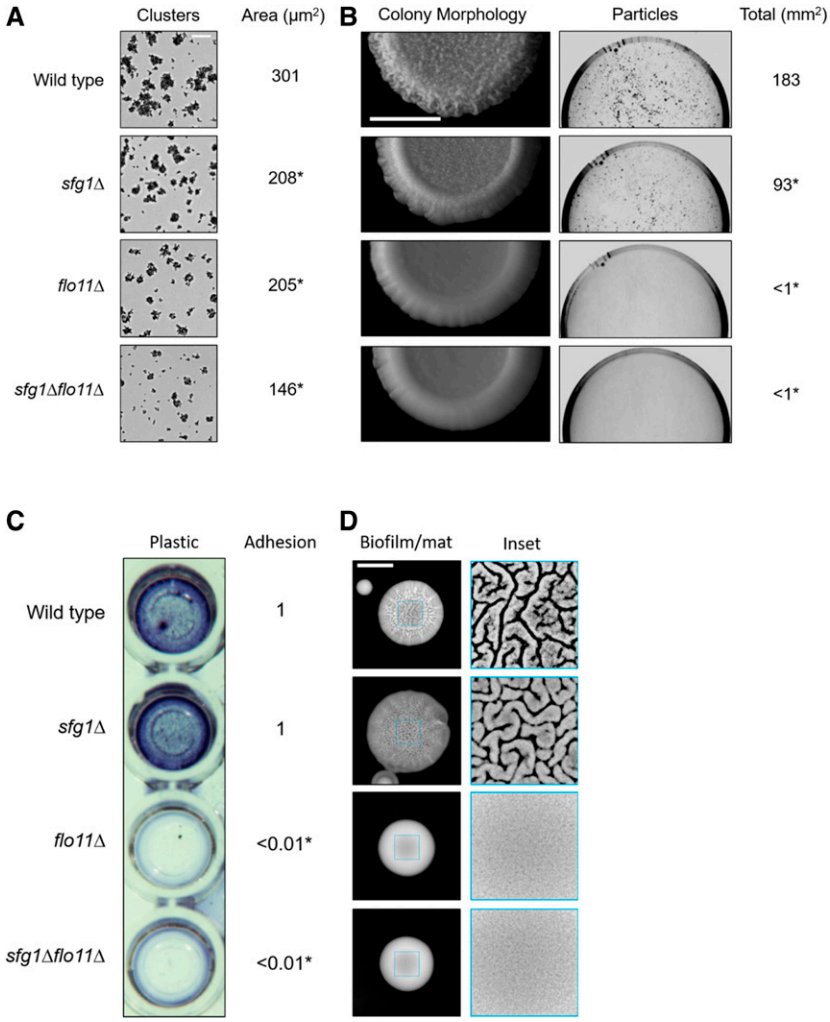

Figure 5 Sfg1p and Flo11p affect cell adhesion differently. (A) Clusters, images of wild-type (PC538) and the *sfg1*Δ (PC7144), *flo11*Δ (PC1029), and *sfg1*Δ*flo11*Δ (PC7280) mutant cells grown in YP-Gal (2%) liquid medium for 24 hr at 5× magnification, Bar, 50 μm. Area (μm²), area quantification for the average size of cell clusters by ImageJ. Error represents SEM which varied < 10% across three trials. Asterisks, *P*-value < 0.05, by Student's *t*-test with wild type. (B) Colony morphology, close up of colony for indicated strains after 6 days on YP-Gal (2%), Bar, 0.5 cm. Particles, adhesive particles from the colony surface. Colonies were grown on YP-Gal (2%) for 3 days, then colony was scraped into dH_2O, mixed, and imaged. Black particles represent groups of cells that remained adherent after mixing. Total, the total area of adherent particles for one colony (mm²) quantified by ImageJ in triplicate. Error represents the SEM and was <10% across three trials. Asterisk, *P*-value <0.005, by Student's *t*-test with wild type. (C) Plastic, adherence estimated by cell adherence to a polystyrene plastic 96-well plate. Indicated strains grown on YP-Gal (2%) medium for 3 days. Cells were scraped from the medium, added to wells, and stained with crystal violet dye. Wells were washed 5× with water. Adhesion, quantification of plastic adhesion by ImageJ in triplicate, with wild-type values set to 1. Error represents the SD, which varied <20% across trials. Asterisks, *P*-value <0.0001, by Student's *t*-test compared to wild type. (D) Biofilm/mat, cells were spotted onto 0.3% agar YP-Gal (2%) for 3 days and imaged. Bar, 1 cm. Inset, close up of biofilm/mat (blue square) to highlight colony pattern.

invasive in the ring region (orange arrows) and just outside of the ring region (green arrows) than the *flo11*Δ mutant. Thus, in these regions Flo11p plays a bigger role in invasive growth than Sfg1p. Along the periphery of the invasive scar, the *flo11*Δ mutant was more invasive than the *sfg1*Δ mutant (Figure 4, A and B, YP-Gal (2%), purple arrows), indicating that in this region, Sfg1p plays a bigger role in invasive growth than Flo11p. Surprisingly, the *flo11*Δ mutant was more invasive than wild type at the periphery (purple arrows). Thus, colonies do not invade in an 'all or none' manner. Rather, cells in different parts of the colony show different levels of invasion that are differentially regulated by Sfg1p and Flo11p.

Many adhesion-dependent responses are regulated by the fMAPK pathway (Chow *et al.* 2019b). For example, cells can form adherent flocs in liquid culture (Verstrepen *et al.* 2003; Halme *et al.* 2004; Fidalgo *et al.* 2006; Barua *et al.* 2016). To examine the role of Sfg1p and Flo11p in this aspect of cell adhesion, we developed an assay to quantify cell adhesion in liquid cultures. This was done by measuring the average area of a group (cluster) of adherent cells by ImageJ after growth in liquid YP-GAL (2%) medium for 24 hr. The *flo11*Δ and *sfg1*Δ single mutants showed a defect in forming clusters (Figure 5A). The *sfg1*Δ *flo11*Δ double mutant showed a more severe defect. Thus, Sfg1p and Flo11p contribute equally in regulating cell adhesion in liquid.

Environmental impacts on Sfg1p- and Flo11p-mediated adhesion

Other adhesion-dependent responses require Flo11p, such as complex colony morphology, where patterns/ruffles form on the colony surface (Granek and Magwene 2010; Karunanithi *et al.* 2012; Chow *et al.* 2019b). The *sfg1*Δ mutant had an intermediate complex colony morphology phenotype between wild-type cells and the *flo11*Δ mutant (Figure 5B, Colony Morphology). By this criterion, the *sfg1*Δ *flo11*Δ double mutant was indistinguishable from the *flo11*Δ mutant. To further investigate this cell-adhesion phenotype, we developed an assay to quantify cell adhesion within colonies. Cells were scraped from the surface of colonies grown on semisolid agar medium, resuspended in dH_2O and mixed. Particles made up of adherent cells were imaged and quantified as

the area of all particles (total) per colony. Cells derived from wild-type colonies formed particles that were visible to the eye, while cells of the *flo11*Δ mutant separated and were not visible by eye [Figure 5B, Particles and Total]. The *sfg1*Δ mutant had an intermediate phenotype (Figure 5B, Particles and Total). The *sfg1*Δ *flo11*Δ double mutant was indistinguishable from the *flo11*Δ mutant by this assay. Thus, Sfg1p plays a minor role compared to Flo11p in this adhesion-dependent phenotype. This is different from the role of Sfg1p in invasive growth and adhesion in liquid where it played the same role as Flo11p.

Some species of yeast, such as *C. albicans*, are pathogens whose adhesion-related behaviors promote virulence. For example, many species of fungi, including pathogens, form biofilms or mats (Lo *et al.* 1997; Reynolds and Fink 2001; Kabir *et al.* 2012; Karunanithi *et al.* 2012; Silva-Dias *et al.* 2015). Biofilm/mats occur when cells adhere together in a complex multicellular community (Costerton *et al.* 1999; Reynolds and Fink 2001; Flemming and Wingender 2010; Kabir *et al.* 2012; Karunanithi *et al.* 2012; Azeredo *et al.* 2017). In this growth mode, cells can adhere to inert surfaces, like plastics, which occurs on medical devices and hospital settings (Kennedy *et al.* 1989; Reynolds and Fink 2001; Kabir *et al.* 2012; Karunanithi *et al.* 2012; Silva-Dias *et al.* 2015). Biofilm/mat formation and plastic adhesion also occur in *S. cerevisiae*, and requires Flo11p [Figure 5, C and D, (Reynolds and Fink 2001; Karunanithi *et al.* 2012)]. Sfg1p was not required for plastic adhesion (Figure 5C) or biofilm/mat expansion and ruffling (Figure 5D). This result indicates Sfg1p is required for a subset of Flo11p-dependent cell-adhesion phenotypes. To summarize, depending on the cell-adhesion phenotype, Sfg1p contributes equally to cell adhesion compared to Flo11p, contributes less, or does not contribute at all.

We also asked whether the environment might impact the way that Sfg1p and Flo11p regulate invasive growth. Compared to YP-GAL (2%), on YPD (2% Glu) medium, the *sfg1*Δ mutant was only slightly defective for invasive growth, whereas the *flo11*Δ mutant was more defective [Figure 4A, YPD (2% Glu), the complete data set is in Figure S6B]. The difference in invasive growth was also evident in the invasive patterns. In particular, the *flo11*Δ mutant was less invasive than the *sfg1*Δ mutant across the entire plot profile [Figure 4B, YPD (2% Glu), compare red and black lines]. The *sfg1*Δ *flo11*Δ double mutant showed no invasive growth on YPD (2% Glu) [Figure 4, A and B, compare the yellow lines in GLU and GAL], indicating that Sfg1p and Flo11p solely control invasive growth under this condition. Furthermore, Flo11p showed different requirements in liquid compared to surface growth. In liquid, the *flo11*Δ mutant had a ∼1.5-fold decrease in adhesion, compared to ∼183-fold decrease on semisolid agar medium (Figure 5A, Area, and Figure 5B, Total). Sfg1p regulated cell adhesion in liquid and on semisolid agar media similarly, because the *sfg1*Δ mutant showed ∼twofold decrease under both conditions (Figure 5A, Area, and Figure 5B, Total). Therefore, Sfg1p and Flo11p play different roles in adhesion-dependent responses depending on the environment.

Sfg1p regulates multiple aspects of filamentous growth

Biofilm/mats are embedded in a matrix that is synthesized by the microbial community (Costerton *et al.* 1999; Flemming and Wingender 2010; Kabir *et al.* 2012; Azeredo *et al.* 2017). In *S. cerevisiae*, Flo11p is shed in biofilms/mats into the extracellular milieu (Karunanithi *et al.* 2010). Given that Sfg1p impacts the expression of cell wall enzymes, Sfg1p was tested for a role in regulating Flo11p shedding. A wild-type HA-tagged Flo11p strain (*FLO11*-HA) and a *sfg1*Δ *FLO11*-HA mutant were grown on a nitrocellulose membrane laid on YP-Gal (2%) semisolid medium. The membrane was washed and probed by antibodies for the HA epitope. Flo11p-HA shedding was reduced in the *sfg1*Δ *FLO11*-HA mutant compared to the wild-type *FLO11*-HA strain (Figure 6A). Many transcription factors converge on the *FLO11* promoter (Borneman *et al.* 2006); therefore, Sfg1p might impact Flo11p shedding by regulating expression of the *FLO11* gene. RT-qPCR analysis showed that *FLO11* expression was reduced in the *sfg1*Δ mutant compared to wild-type cells (Figure 6A, *FLO11* expression). Therefore, Sfg1p regulates cell adhesion in part by regulating *FLO11* expression. Sfg1p might also impact Flo11p shedding through cell wall remodeling.

To determine the role of Sfg1p in regulating cell adhesion independent of *FLO11* expression, a strain where *FLO11* is expressed from a galactose-inducible promoter (*GAL-FLO11*) was compared to the *sfg1*Δ *GAL-FLO11* mutant for invasive growth and cluster formation. Overexpression of *FLO11* caused increased invasive growth [Figure 6B, washed, (Chow *et al.* 2019a)] and the formation of large clusters (Figure 6B, Clusters and Area). Deletion of *SFG1* in the *GAL-FLO11* strain led to a decrease in invasive growth and a reduction in cluster size (Figure 6B). This data indicates that Sfg1p primarily regulates cell adhesion independent of *FLO11* expression. As shown above, Sfg1p had no effect on some Flo11p-dependent responses, like biofilm/mat formation and plastic adhesion. Thus, Sfg1p might not regulate *FLO11* expression under all conditions. This idea is supported by the fact that Sfg1p did not regulate Flo11p shedding under all conditions (Figure S7).

In addition to cell adhesion, cells undergoing filamentous growth also regulate cell elongation. Cells elongate by a delay in the cell cycle that leads to extended apical growth (Kron *et al.* 1994; Edgington *et al.* 1999). The fMAPK pathway causes a delay in the cell cycle by inducing expression of the *CLN1* gene (Loeb *et al.* 1999; Madhani *et al.* 1999), which encodes a G_1/S specific cyclin (Hadwiger *et al.* 1989). However, this is not the only way the fMAPK pathway induces a delay in the cell cycle (Ahn *et al.* 1999). One additional way may be through regulating the expression of *SFG1* because *SFG1* regulates the cell cycle (White *et al.* 2009). A *sfg1*Δ mutant is delayed in the G_1 phase of the cell cycle, and *SFG1* overexpression causes a delay in G_2/M (White *et al.*

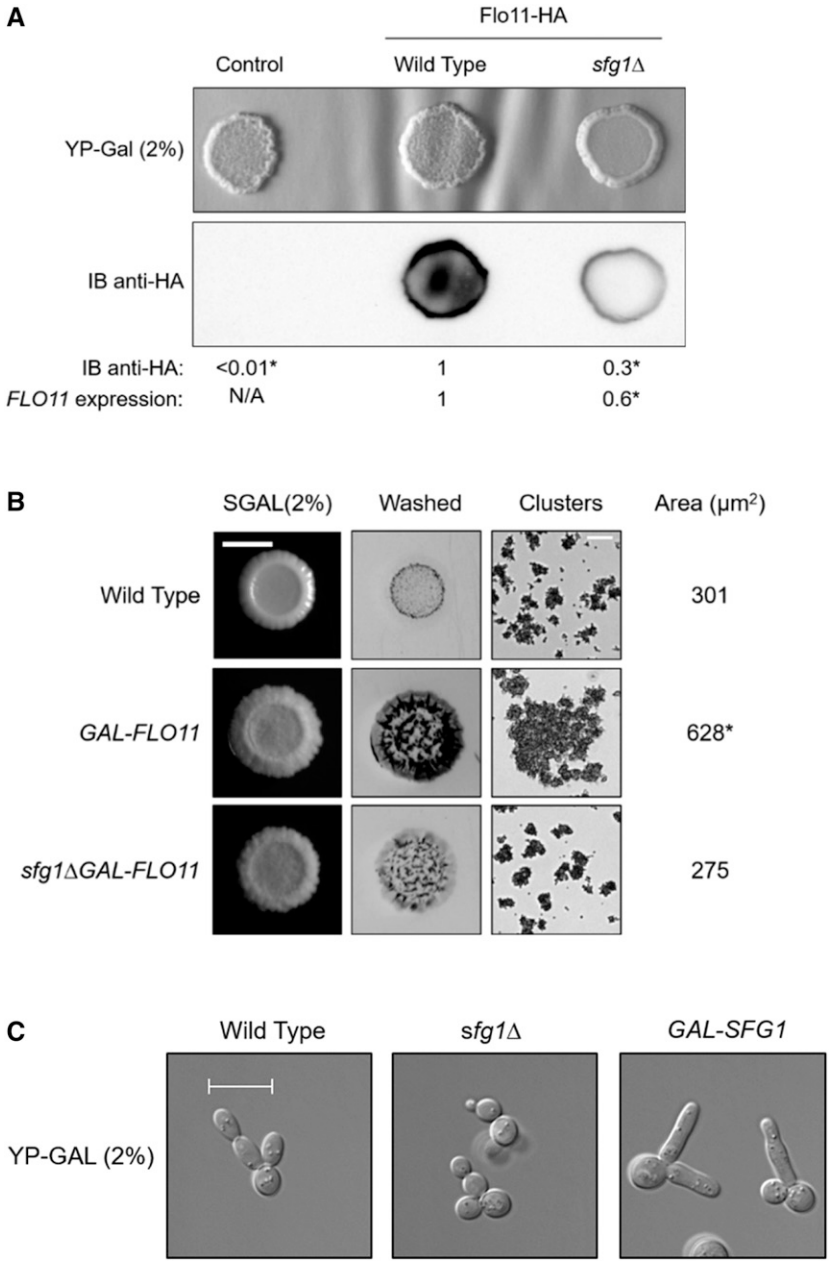

Figure 6 Sfg1p regulates *FLO11* expression and cell elongation. (A) Colony immunoblot to detect HA-Flo11p with anti-HA antibodies. Wild type (PC538), *FLO11*-HA (PC2043), and *sfg1*Δ*FLO11*-HA (PC7321) strains were grown on nitrocellulose membranes atop YP-Gal (2%) semisolid agar medium for 3 days. Numbers refer to the intensity of anti-HA quantified by image lab. Experiments were performed in triplicate. Error is SEM with <20% variation across trials. Asterisks, *P*-value <0.02, by Student's *t*-test compared to wild type. *FLO11* expression, fold change in *FLO11* mRNA levels by RT-qPCR analysis normalized to *ACT1*, wild-type values set to 1. *FLO11* expression was measured in wild-type (PC538) and *sfg1*Δ (PC7144) strains. Error represents SD, which varied <30% across trials. Asterisks, *P*-value <0.03, by Student's *t*-test with wild type. (B) Left and middle columns, Plate-washing assay for wild type (PC538), Gal-*FLO11* (PC2712) *sfg1*ΔGal-*FLO11* (PC7281) strains on SGAL+AA after 6 days. Left column, before wash and middle column, after wash, Bar, 0.5 cm. Right column, images of cells grown in YP-Gal (2%) liquid medium for 24 hr imaged at 5× magnification, Bar, 50 μm. Area values represent ImageJ quantification for the average size of cell clusters by area (μm²) for indicated strains. Error represents SEM which varied <15% across three trials. Asterisk, *P*-value = 0.01, by Student's *t*-test with wild type. Wild-type data are from Figure 3. (C) Cell morphology compared after growth in YP-Gal (2%) for 4 hr between wild-type cells (PC538), *sfg1*Δ (PC7144), and wild type transformed with a plasmid containing an overexpression of *SFG1* by a galactose-inducible promoter (pGAL-SFG1). Bar, 10 μm.

2009). We found by microscopy, the *sfg1*Δ mutant had a round-cell morphology compared to wild-type cells, and overexpression of *SFG1* by a galactose-inducible promoter [p*GAL-SFG1* (Gelperin *et al.* 2005)] induced an elongated morphology (Figure 6C). Thus, the fMAPK pathway may regulate cell elongation by multiple mechanisms, such as by controlling the expression of the *CLN1* and *SFG1* genes.

Sfg1p was previously shown to be a distantly related member of a family of transcriptional regulators of fungal development in nonpathogenic and pathogenic fungi because it has weak similarity in protein sequence to a family of transcription factors involved in pseudohyphal/hyphal development (Fujita *et al.* 2005). These include Phd1p and Sok2p in *S. cerevisiae* (Gimeno and Fink 1994; Ward *et al.* 1995; Fujita *et al.* 2005); Efg1p in *C. albicans* (Stoldt *et al.* 1997; Fujita *et al.* 2005); StuA in *Aspergillus nidulans* (Miller *et al.* 1992; Fujita *et al.* 2005); and Asm-1 in *Neurospora crassa* (Aramayo *et al.* 1996; Fujita *et al.* 2005). We found that *SFG1* shows synteny (by the Yeast Gene Order browser) and protein sequence similarity (by BLAST) to other fungi species as well (Figure S5, A and B), including an uncharacterized ORF (CAGL0I09856g) in the human pathogen *C. glabrata* (Fidel *et al.* 1999; Csank and Haynes 2000; Rodrigues *et al.* 2014). Presumably, *SFG1* is required for filamentous growth in other fungal species besides *S. cerevisiae*, and may be an important regulator in some pathogenic yeasts.

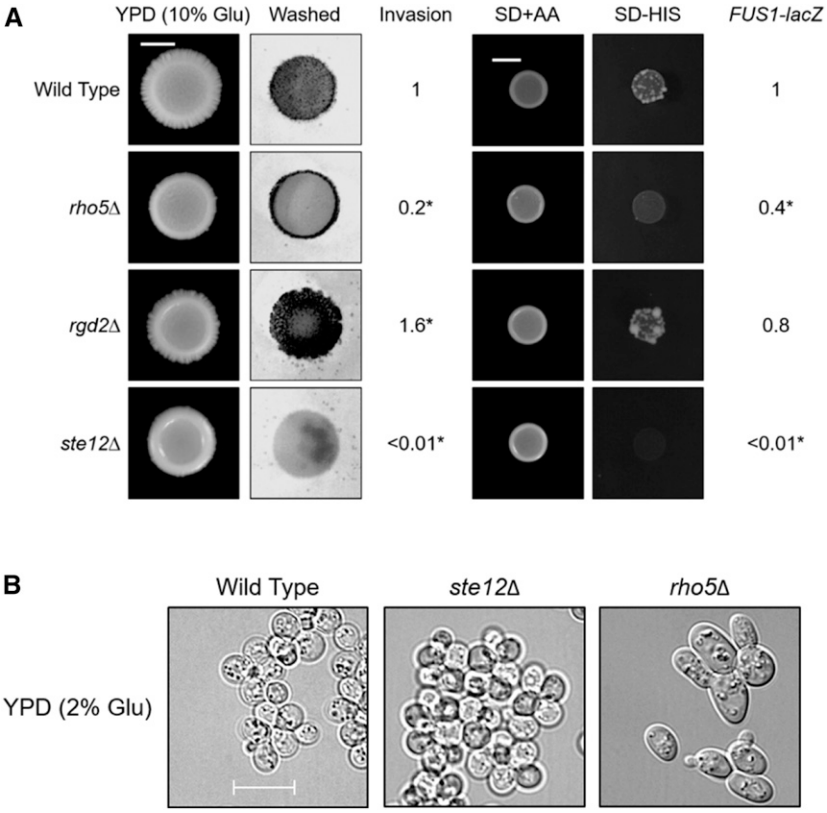

Figure 7 Rho5p regulates the fMAPK pathway. (A) Plate-washing assay of wild type (PC538+pRS316) and the *rho5*Δ (PC7306), *rgd2*Δ (PC7146), and *ste12*Δ (PC539) mutants spotted on YPD (10% Glu) and grown for 3 days. Left column, colonies, second column, inverted images of plates after wash, Bar, 0.5 cm. Invasion, quantification of invasive scars by ImageJ in triplicate, with wild type values set to 1. Error represents the SEM, which varied ≤ 50% across three trials. Asterisks, *P*-value < 0.035, by Student's *t*-test compared to wild type. The *rgd2*Δ mutant invasion value is from Figure 2. SD+AA, strains spotted onto SD+AA and grown for 3 days. SD-HIS, transcriptional (growth) reporter [*FUS1-HIS3*]. Strains grown on SD-HIS+ATA (3-amino-1,2,4-triazole) medium for 3 days. *FUS1-lacZ*, β-Galactosidase (*lacZ*) assays. Cells grown in SD-URA for 16 hr, washed, and resuspended in YPD (10% Glu) medium for 6.5 hr prior to harvesting cells by centrifugation. Error represents SEM, which varied < 10% across three trials. Asterisk, *P*-value < 0.01. (B) Cell morphology compared after growth in YPD (2% Glu) for 16 hr between indicated strains. Bar, 10 μm.

RHO5 regulates the activity of the fMAPK pathway

Rho5p is a small GTPase of the Rho family (Garcia-Ranea and Valencia 1998; Singh *et al.* 2008, 2019; Schmitz *et al.* 2018). *RHO5* was not a target of the fMAPK pathway; however, it is regulated by the GTPase-activating protein Rgd2p (Annan *et al.* 2008), which was a target of the fMAPK pathway (Figure 1B). The plate-washing assay showed that the *rho5*Δ mutant was defective for invasive growth (Figure 7A, Washed and Invasion) supporting previous observations (Ryan *et al.* 2012; Foster *et al.* 2013). To explore if Rho5p regulates invasive growth through the fMAPK pathway, the *rho5*Δ mutant was tested for fMAPK pathway activity by a transcriptional (growth) reporter [*FUS1-HIS3*] and a *lacZ* reporter [*FUS1-lacZ*]. Both reporters reflect the activity of the fMAPK pathway in cells lacking an intact mating pathway [*ste4*Δ (Cullen *et al.* 2004)]. The *rho5*Δ mutant was defective for fMAPK pathway activity based on growth on SD-HIS media (Figure 7A, SD-HIS). This was not due to a growth defect on synthetic media (Figure 7A, SD+AA). The fMAPK pathway also showed reduced activity in the *rho5*Δ mutant by the *FUS1-lacZ* reporter (Figure 7A, *FUS1-lacZ*). These results indicate that Rho5p may play a subtle role in regulating the fMAPK pathway. We did not find a link between Rgd2p and Rho5p in the regulation of the fMAPK pathway because the *rgd2*Δ mutant, unlike the *rho5*Δ mutant, did not show a change in fMAPK pathway activity by the *FUS1-HIS3* or the *FUS1-lacZ* reporters (Figure 7A). By microscopy, the *rho5*Δ mutant also showed misshaped cell morphology and improper budding (Figure 7B). Overall, the data establishes Rho5p as a positive regulator of the fMAPK pathway.

Discussion

Signaling pathways can regulate the activity of transcription factors that control the expression of many genes that collectively generate cellular responses. To have a full understanding of the cellular responses a pathway generates, one must characterize the functions of its individual targets of the signaling pathway. Here, we characterized targets of the fMAPK pathway in *S. cerevisiae*. This led to the discovery that, even though the fMAPK pathway overwhelmingly regulates filamentous growth positively, the pathway can also negatively regulate or modulate filamentous growth under some conditions. This also led to the discovery of new positive roles for the pathway in controlling cell adhesion and the cell cycle (Figure 8). In addition, by trying to identify how the target *RGD2* regulates invasive growth, we uncovered that *RHO5* positively regulates the fMAPK pathway (Figure 8).

A major role of the fMAPK pathway is to positively regulate invasive growth (Roberts and Fink 1994; Cook *et al.* 1997; Roberts *et al.* 2000; Cullen and Sprague 2012). Here, we show that the fMAPK pathway also negatively regulates invasive growth. This occurred under certain conditions by regulating the expression of *NFG1*, *RGD2*, *RPI1*, and *TIP1*. Moreover, the fMAPK pathway induces the expression of

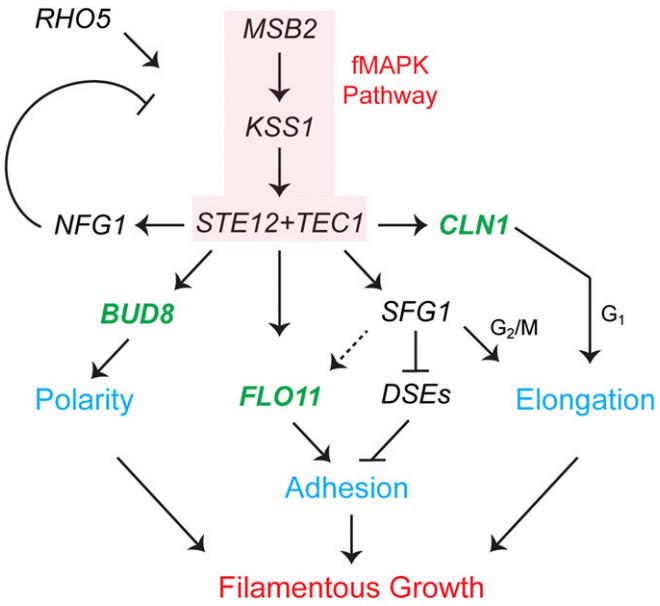

Figure 8 Model of how newly identified targets of the fMAPK pathway impact cell adhesion and cell elongation during filamentous growth. Nfg1p negatively regulates the fMAPK pathway. Other targets also negatively regulate filamentous growth (not shown). The fMAPK pathway induces cell adhesion by regulating *FLO11* expression, in part through Sfg1p, and by preventing cell separation through Sfg1p-dependent repression of *DSEs* and *SCW11*. The fMAPK pathway induces cell elongation by regulating the G_1-specific cyclin *CLN1* and *SFG1*, which promotes extension of G_2/M. Rho5p regulates the fMAPK pathway. Pathway components are highlighted in red (*MSB2*, *KSS1*, *STE12*, *TEC1*).

these negative regulators to modulate the formation of invasive aggregates. This adds four new proteins to the large group of proteins that negatively regulate filamentous growth, including Sfl1p (Fujita *et al.* 1989; Robertson and Fink 1998; Song and Carlson 1998; Pan and Heitman 2002), Nrg1p (Park *et al.* 1999; Zhou and Winston 2001; Kuchin *et al.* 2002), Sok2p (Ward *et al.* 1995; Pan and Heitman 2000, 2002), and Dig1p (Cook *et al.* 1996; Tedford *et al.* 1997; Bardwell *et al.* 1998b; Olson *et al.* 2000). Rgd2p, Rpi1p, and Tip1p are conserved in several yeast species, including pathogens, and might have similar functions in these species. Nfg1p, however, only has homology within *Saccharomyces* yeast. Perhaps Nfg1p aids in a specific aspect of *Saccharomyces* ecology not found in other fungi.

Because the fMAPK pathway is involved in both the negative and positive regulation of filamentous growth, it implies the importance of fine tuning in the regulation of this response. Modulation ensures cells do not "overdo" filamentous growth, which, in some environments, could have negative impacts. For example, when Dig1p is overexpressed, it gives cells a growth advantage in liquid cultures, but reduces growth on semisolid surfaces (Tan *et al.* 2013). Furthermore, a *dig1*Δ mutant has decreased biofilm/mat expansion (Karunanithi *et al.* 2012), which could make it more difficult to scavenge nutrients. Finally, elevated levels of Flo11p, although beneficial for invasive growth, dampens biofilm/mat expansion (Karunanithi *et al.* 2010).

Nfg1p has been an established, highly induced target of the fMAPK pathway with a function that has remained elusive for some time [*YLR042c*, (Caro *et al.* 1997; Hamada *et al.* 1999; Madhani *et al.* 1999; Roberts *et al.* 2000; Giaever *et al.* 2002; Hohmann 2002; García *et al.* 2004; Kim and Levin 2010; Parachin *et al.* 2010; Adhikari and Cullen 2014; Chow *et al.* 2019b)]. Here, we show Nfg1p regulates invasive growth by dampening the activity of the fMAPK pathway (Figure 8). This fits a common theme among some pathway targets that are induced to dampen pathway activity, resulting in negative feedback (Borneman *et al.* 2006). Rgd2p, Rpi1p, and Tip1p act at least somewhat separately from Nfg1p and each other to modulate invasive growth. Rgd2p, Rpi1p, and Tip1p may dampen other pathways that regulate filamentous growth (Gimeno *et al.* 1992; Lorenz and Heitman 1998; Carlson 1999; Pan and Heitman 1999; Cullen and Sprague 2000, 2012; Crespo *et al.* 2002; Lamb and Mitchell 2003) because extensive cross regulation between pathways occurs in a complex regulatory network (Bharucha *et al.* 2008; Chavel *et al.* 2010, *et al.*2014; Chow *et al.* 2019b). As currently appreciated, it is not clear how signal amplification is curbed in the network. Here, we provide a possible explanation for this, by pathways making products that presumably dampen the activity of other pathways from the signaling network. For example, the fMAPK pathway may target *RPI1* because it dampens the Ras/cyclic AMP pathway (Kim and Powers 1991; Sobering *et al.* 2002), which also regulates filamentous growth (Mosch *et al.* 1996; Pan and Heitman 1999; Rupp *et al.* 1999; Cullen and Sprague 2012).

We also show that the transcriptional repressor *SFG1* is a target of the fMAPK pathway. Sfg1p regulates an entire filamentation program—it prevents cell separation by repressing genes encoding daughter-cell-wall degrading enzymes, it triggers cell cycle delay resulting in an elongated cell morphology, and it induces *FLO11* expression (Figure 8). Sfg1p also regulates cell adhesion separate from Flo11p. Thus, the regulation of *SFG1* expression by the fMAPK pathway identifies a new mechanism by which the fMAPK pathway regulates cell adhesion. Sfg1p and Flo11p do not always contribute equally to cell-adhesion responses, and cell-adhesion regulation by both proteins was affected by the environment. Flo11p regulated cell adhesion more intensely on semisolid than in liquid media, and both Sfg1p and Flo11p regulated invasive growth differently depending on the carbon source present. These new conditional mechanisms indicate that cell adhesion regulation is more complex than currently appreciated and suggests that, in yeast, there is an 'adhesion code'. For example, we show here that the adhesion code is dependent on the regulation of adhesion molecules, cell-wall-degrading enzymes, and transcription factors, which are controlled differentially depending on the environment. Given the large number of adhesion molecules in *C. albicans* and other species (Tronchin *et al.* 1991; Brandhorst *et al.* 1999;

Sheppard *et al.* 2004; Dranginis *et al.* 2007; Linder and Gustafsson 2008; Younes *et al.* 2011; de Groot *et al.* 2013; Lipke 2018; Takahashi-Nakaguchi *et al.* 2018), it is likely that the adhesion code in other species is similarly (or more) complex.

Sfg1p also regulated cell elongation, and based on previous work has been shown to induce a delay in G_2/M (White *et al.* 2009). Overall, it appears the fMAPK pathway integrates separate regulatory modes of filamentous growth into one response: (1) regulating cell adhesion by repressing the expression of genes that encode proteins involved in cell separation and inducing the expression of *FLO11* and (2) regulating the cell cycle at G_1 through *CLN1* and G_2 through *SFG1* to promote cell elongation (Figure 8). Having multiple mechanisms to regulate the same response increases the fine tuning capabilities of the pathway, making slight adjustments for different environments possible. Sfg1p is conserved across some species of yeast, including pathogens like *C. glabrata*, and could represent an important regulator of filamentous growth that leads to nuanced responses in other species.

In conclusion, by characterizing transcriptional targets of the fMAPK pathway, we have identified novel roles for the pathway in regulating invasive growth, cell adhesion, and the cell cycle. Some of these mechanisms may be conserved in pathogenic yeasts and could assist in understanding fungal infections. Here, we focused on highly induced targets of the fMAPK pathway; however, there are many other targets genes that are induced at lower levels that could impact phenotype. Moreover, there are also many targets whose expression is repressed that may tell us phenotypic information about the fMAPK pathway if explored. Overall, these findings suggest characterizing the genetic targets of other signaling pathways could lead to important advances in understanding signal transduction regulation.

Acknowledgments

Thanks to Kathryn Vandermeulen, Alexander Bowitch, and past and current laboratory members. The work was supported by a grant from the National Institutes of Health (NIH) (GM098629). The authors have no competing interests in the study.

Author contributions: M.D.V. designed experiments, generated data, and wrote the paper; P.J.C. designed experiments, wrote the paper, and obtained funding.

Literature Cited

Adhikari, H., and P. J. Cullen, 2014 Metabolic respiration induces AMPK- and Ire1p-dependent activation of the p38-Type HOG MAPK pathway. PLoS Genet. 10: e1004734. https://doi.org/10.1371/journal.pgen.1004734

Ahn, S. H., A. Acurio, and S. J. Kron, 1999 Regulation of G2/M progression by the STE mitogen-activated protein kinase pathway in budding yeast filamentous growth. Mol. Biol. Cell 10: 3301–3316. https://doi.org/10.1091/mbc.10.10.3301

Annan, R. B., C. Wu, D. D. Waller, M. Whiteway, and D. Y. Thomas, 2008 Rho5p is involved in mediating the osmotic stress response in Saccharomyces cerevisiae, and its activity is regulated via Msi1p and Npr1p by phosphorylation and ubiquitination. Eukaryot. Cell 7: 1441–1449. https://doi.org/10.1128/EC.00120-08

Aramayo, R., Y. Peleg, R. Addison, and R. Metzenberg, 1996 Asm-1+, a Neurospora crassa gene related to transcriptional regulators of fungal development. Genetics 144: 991–1003.

Azeredo, J., N. F. Azevedo, R. Briandet, N. Cerca, T. Coenye *et al.*, 2017 Critical review on biofilm methods. Crit. Rev. Microbiol. 43: 313–351. https://doi.org/10.1080/1040841X.2016.1208146

Baladrón, V., S. Ufano, E. Duenas, A. B. Martin-Cuadrado, F. del Rey *et al.*, 2002 Eng1p, an endo-1,3-beta-glucanase localized at the daughter side of the septum, is involved in cell separation in Saccharomyces cerevisiae. Eukaryot. Cell 1: 774–786. https://doi.org/10.1128/EC.1.5.774-786.2002

Bardwell, L., J. G. Cook, D. Voora, D. M. Baggott, A. R. Martinez *et al.*, 1998a Repression of yeast Ste12 transcription factor by direct binding of unphosphorylated Kss1 MAPK and its regulation by the Ste7 MEK. Genes Dev. 12: 2887–2898. https://doi.org/10.1101/gad.12.18.2887

Bardwell, L., J. G. Cook, J. X. Zhu-Shimoni, D. Voora, and J. Thorner, 1998b Differential regulation of transcription: repression by unactivated mitogen-activated protein kinase Kss1 requires the Dig1 and Dig2 proteins. Proc. Natl. Acad. Sci. USA 95: 15400–15405. https://doi.org/10.1073/pnas.95.26.15400

Barua, S., L. Li, P. N. Lipke, and A. M. Dranginis, 2016 Molecular basis for strain variation in the Saccharomyces cerevisiae adhesin Flo11p. MSphere 1: e00129–16. https://doi.org/10.1128/mSphere.00129-16

Basu, S., N. Vadaie, A. Prabhakar, B. Li, H. Adhikari *et al.*, 2016 Spatial landmarks regulate a Cdc42-dependent MAPK pathway to control differentiation and the response to positional compromise. Proc. Natl. Acad. Sci. USA 113: E2019–E2028. https://doi.org/10.1073/pnas.1522679113

Basu, S., B. Gonzalez, B. Li, G. Kimble, K. G. Kozminski *et al.*, 2020 Functions for Cdc42p BEM adaptors in regulating a differentiation-type MAP kinase pathway. Mol. Biol. Cell 31: 491–510. https://doi.org/10.1091/mbc.E19-08-0441

Bharucha, N., J. Ma, C. J. Dobry, S. K. Lawson, Z. Yang *et al.*, 2008 Analysis of the yeast kinome reveals a network of regulated protein localization during filamentous growth. Mol. Biol. Cell 19: 2708–2717. https://doi.org/10.1091/mbc.e07-11-1199

Birkaya, B., A. Maddi, J. Joshi, S. J. Free, and P. J. Cullen, 2009 Role of the cell wall integrity and filamentous growth mitogen-activated protein kinase pathways in cell wall remodeling during filamentous growth. Eukaryot. Cell 8: 1118–1133. https://doi.org/10.1128/EC.00006-09

Borneman, A. R., J. A. Leigh-Bell, H. Yu, P. Bertone, M. Gerstein *et al.*, 2006 Target hub proteins serve as master regulators of development in yeast. Genes Dev. 20: 435–448. https://doi.org/10.1101/gad.1389306

Borneman, A. R., Z. D. Zhang, J. Rozowsky, M. R. Seringhaus, M. Gerstein *et al.*, 2007 Transcription factor binding site identification in yeast: a comparison of high-density oligonucleotide and PCR-based microarray platforms. Funct. Integr. Genomics 7: 335–345. https://doi.org/10.1007/s10142-007-0054-7

Brandhorst, T. T., M. Wuthrich, T. Warner, and B. Klein, 1999 Targeted gene disruption reveals an adhesin indispensable for pathogenicity of Blastomyces dermatitidis. J. Exp. Med. 189: 1207–1216. https://doi.org/10.1084/jem.189.8.1207

Brito, A. S., B. Neuhauser, R. Wintjens, A. M. Marini, and M. Boeckstaens, 2020 Yeast filamentation signaling is connected to a specific substrate translocation mechanism of the Mep2

transceptor. PLoS Genet. 16: e1008634. https://doi.org/10.1371/journal.pgen.1008634
Brückner, S., R. Schubert, T. Kraushaar, R. Hartmann, D. Hoffmann *et al.*, 2020 Kin discrimination in social yeast is mediated by cell surface receptors of the Flo11 adhesin family. eLife 9: e55587. https://doi.org/10.7554/eLife.55587
Byrne, K. P., and K. H. Wolfe, 2005 The Yeast Gene Order Browser: combining curated homology and syntenic context reveals gene fate in polyploid species. Genome Res. 15: 1456–1461. https://doi.org/10.1101/gr.3672305
Byrne, K. P., and K. H. Wolfe, 2006 Visualizing syntenic relationships among the hemiascomycetes with the yeast gene order browser. Nucleic Acids Res. 34: D452–D455. https://doi.org/10.1093/nar/gkj041
Carlson, M., 1999 Glucose repression in yeast. Curr. Opin. Microbiol. 2: 202–207. https://doi.org/10.1016/S1369-5274(99)80035-6
Carlson, M., B. C. Osmond, and D. Botstein, 1981 Mutants of yeast defective in sucrose utilization. Genetics 98: 25–40.
Caro, L. H., H. Tettelin, J. H. Vossen, A. F. Ram, H. van den Ende *et al.*, 1997 In silicio identification of glycosyl-phosphatidylinositol-anchored plasma-membrane and cell wall proteins of Saccharomyces cerevisiae. Yeast 13: 1477–1489. https://doi.org/10.1002/(SICI)1097-0061(199712)13:15<1477::AID-YEA184>3.0.CO;2-L
Chang, L., and M. Karin, 2001 Mammalian MAP kinase signalling cascades. Nature 410: 37–40. https://doi.org/10.1038/35065000
Chavel, C. A., H. M. Dionne, B. Birkaya, J. Joshi, and P. J. Cullen, 2010 Multiple signals converge on a differentiation MAPK pathway. PLoS Genet. 6: e1000883. https://doi.org/10.1371/journal.pgen.1000883
Chavel, C. A., L. M. Caccamise, B. Li, and P. J. Cullen, 2014 Global regulation of a differentiation MAPK pathway in yeast. Genetics 198: 1309–1328. https://doi.org/10.1534/genetics.114.168252
Chen, H., and G. R. Fink, 2006 Feedback control of morphogenesis in fungi by aromatic alcohols. Genes Dev. 20: 1150–1161. https://doi.org/10.1101/gad.1411806
Chin, B. L., O. Ryan, F. Lewitter, C. Boone, and G. R. Fink, 2012 Genetic variation in Saccharomyces cerevisiae: circuit diversification in a signal transduction network. Genetics 192: 1523–1532. https://doi.org/10.1534/genetics.112.145573
Chou, S., S. Lane, and H. Liu, 2006 Regulation of mating and filamentation genes by two distinct Ste12 complexes in Saccharomyces cerevisiae. Mol. Cell. Biol. 26: 4794–4805. https://doi.org/10.1128/MCB.02053-05
Chow, J., M. Notaro, A. Prabhakar, S. J. Free, and P. J. Cullen, 2018 Impact of fungal MAPK pathway targets on the cell wall. J. Fungi (Basel) 4: 93. https://doi.org/10.3390/jof4030093
Chow, J., H. M. Dionne, A. Prabhakar, A. Mehrotra, J. Somboonthum *et al.*, 2019a Aggregate filamentous growth responses in yeast. MSphere 4: e00702–18. https://doi.org/10.1128/mSphere.00702-18
Chow, J., I. Starr, S. Jamalzadeh, O. Muniz, A. Kumar *et al.*, 2019b Filamentation regulatory pathways control adhesion-dependent surface responses in yeast. Genetics 212: 667–690. https://doi.org/10.1534/genetics.119.302004
Cook, J. G., L. Bardwell, S. J. Kron, and J. Thorner, 1996 Two novel targets of the MAP kinase Kss1 are negative regulators of invasive growth in the yeast Saccharomyces cerevisiae. Genes Dev. 10: 2831–2848. https://doi.org/10.1101/gad.10.22.2831
Cook, J. G., L. Bardwell, and J. Thorner, 1997 Inhibitory and activating functions for MAPK Kss1 in the S. cerevisiae filamentous-growth signalling pathway. Nature 390: 85–88. https://doi.org/10.1038/36355
Costanzo, M., A. Baryshnikova, J. Bellay, Y. Kim, E. D. Spear *et al.*, 2010 The genetic landscape of a cell. Science 327: 425–431. https://doi.org/10.1126/science.1180823
Costerton, J. W., P. S. Stewart, and E. P. Greenberg, 1999 Bacterial biofilms: a common cause of persistent infections. Science 284: 1318–1322. https://doi.org/10.1126/science.284.5418.1318
Courchesne, W. E., R. Kunisawa, and J. Thorner, 1989 A putative protein kinase overcomes pheromone-induced arrest of cell cycling in S. cerevisiae. Cell 58: 1107–1119. https://doi.org/10.1016/0092-8674(89)90509-6
Craig Maclean, R., and C. Brandon, 2008 Stable public goods cooperation and dynamic social interactions in yeast. J. Evol. Biol. 21: 1836–1843. https://doi.org/10.1111/j.1420-9101.2008.01579.x
Crespo, J. L., T. Powers, B. Fowler, and M. N. Hall, 2002 The TOR-controlled transcription activators GLN3, RTG1, and RTG3 are regulated in response to intracellular levels of glutamine. Proc. Natl. Acad. Sci. USA 99: 6784–6789. https://doi.org/10.1073/pnas.102687599
Csank, C., and K. Haynes, 2000 Candida glabrata displays pseudohyphal growth. FEMS Microbiol. Lett. 189: 115–120. https://doi.org/10.1111/j.1574-6968.2000.tb09216.x
Cullen, P. J., 2015 The plate-washing assay: a simple test for filamentous growth in budding yeast. Cold Spring Harb. Protoc. 2015: 168–171. https://doi.org/10.1101/pdb.prot085068
Cullen, P. J., and G. F. Sprague, Jr., 2000 Glucose depletion causes haploid invasive growth in yeast. Proc. Natl. Acad. Sci. USA 97: 13619–13624. https://doi.org/10.1073/pnas.240345197
Cullen, P. J., and G. F. Sprague, Jr., 2002 The roles of bud-site-selection proteins during haploid invasive growth in yeast. Mol. Biol. Cell 13: 2990–3004. https://doi.org/10.1091/mbc.e02-03-0151
Cullen, P. J., and G. F. Sprague, Jr., 2012 The regulation of filamentous growth in yeast. Genetics 190: 23–49. https://doi.org/10.1534/genetics.111.127456
Cullen, P. J., J. Schultz, J. Horecka, B. J. Stevenson, Y. Jigami *et al.*, 2000 Defects in protein glycosylation cause SHO1-dependent activation of a STE12 signaling pathway in yeast. Genetics 155: 1005–1018.
Cullen, P. J., W. Sabbagh, Jr., E. Graham, M. M. Irick, E. K. van Olden *et al.*, 2004 A signaling mucin at the head of the Cdc42- and MAPK-dependent filamentous growth pathway in yeast. Genes Dev. 18: 1695–1708. https://doi.org/10.1101/gad.1178604
de Groot, P. W., O. Bader, A. D. de Boer, M. Weig, and N. Chauhan, 2013 Adhesins in human fungal pathogens: glue with plenty of stick. Eukaryot. Cell 12: 470–481. https://doi.org/10.1128/EC.00364-12
Doolin, M. T., A. L. Johnson, L. H. Johnston, and G. Butler, 2001 Overlapping and distinct roles of the duplicated yeast transcription factors Ace2p and Swi5p. Mol. Microbiol. 40: 422–432. https://doi.org/10.1046/j.1365-2958.2001.02388.x
Dranginis, A. M., J. M. Rauceo, J. E. Coronado, and P. N. Lipke, 2007 A biochemical guide to yeast adhesins: glycoproteins for social and antisocial occasions. Microbiol. Mol. Biol. Rev. 71: 282–294. https://doi.org/10.1128/MMBR.00037-06
Draper, E., O. Dubrovskyi, E. E. Bar, and D. E. Stone, 2009 Dse1 may control cross talk between the pheromone and filamentation pathways in yeast. Curr. Genet. 55: 611–621. https://doi.org/10.1007/s00294-009-0274-6
Edgington, N. P., M. J. Blacketer, T. A. Bierwagen, and A. M. Myers, 1999 Control of Saccharomyces cerevisiae filamentous growth by cyclin-dependent kinase Cdc28. Mol. Cell. Biol. 19: 1369–1380. https://doi.org/10.1128/MCB.19.2.1369

Fidalgo, M., R. R. Barrales, J. I. Ibeas, and J. Jimenez, 2006 Adaptive evolution by mutations in the FLO11 gene. Proc. Natl. Acad. Sci. USA 103: 11228–11233. https://doi.org/10.1073/pnas.0601713103

Fidel, Jr., P. L., J. A. Vazquez, and J. D. Sobel, 1999 Candida glabrata: review of epidemiology, pathogenesis, and clinical disease with comparison to C. albicans. Clin. Microbiol. Rev. 12: 80–96. https://doi.org/10.1128/CMR.12.1.80

Flatauer, L. J., S. F. Zadeh, and L. Bardwell, 2005 Mitogen-activated protein kinases with distinct requirements for Ste5 scaffolding influence signaling specificity in Saccharomyces cerevisiae. Mol. Cell. Biol. 25: 1793–1803. https://doi.org/10.1128/MCB.25.5.1793-1803.2005

Flemming, H. C., and J. Wingender, 2010 The biofilm matrix. Nat. Rev. Microbiol. 8: 623–633. https://doi.org/10.1038/nrmicro2415

Foster, H. A., M. Cui, A. Naveenathayalan, H. Unden, R. Schwanbeck *et al.*, 2013 The zinc cluster protein Sut1 contributes to filamentation in Saccharomyces cerevisiae. Eukaryot. Cell 12: 244–253. https://doi.org/10.1128/EC.00214-12

Fujii, T., H. Shimoi, and Y. Iimura, 1999 Structure of the glucan-binding sugar chain of Tip1p, a cell wall protein of Saccharomyces cerevisiae. Biochim. Biophys. Acta 1427: 133–144. https://doi.org/10.1016/S0304-4165(99)00012-4

Fujita, A., Y. Kikuchi, S. Kuhara, Y. Misumi, S. Matsumoto *et al.*, 1989 Domains of the SFL1 protein of yeasts are homologous to Myc oncoproteins or yeast heat-shock transcription factor. Gene 85: 321–328. https://doi.org/10.1016/0378-1119(89)90424-1

Fujita, A., T. Hiroko, F. Hiroko, and C. Oka, 2005 Enhancement of superficial pseudohyphal growth by overexpression of the SFG1 gene in yeast Saccharomyces cerevisiae. Gene 363: 97–104. https://doi.org/10.1016/j.gene.2005.06.036

García, R., C. Bermejo, C. Grau, R. Perez, J. M. Rodriguez-Pena *et al.*, 2004 The global transcriptional response to transient cell wall damage in Saccharomyces cerevisiae and its regulation by the cell integrity signaling pathway. J. Biol. Chem. 279: 15183–15195. https://doi.org/10.1074/jbc.M312954200

Garcia-Ranea, J. A., and A. Valencia, 1998 Distribution and functional diversification of the ras superfamily in Saccharomyces cerevisiae. FEBS Lett. 434: 219–225. https://doi.org/10.1016/S0014-5793(98)00967-3

Gelperin, D. M., M. A. White, M. L. Wilkinson, Y. Kon, L. A. Kung *et al.*, 2005 Biochemical and genetic analysis of the yeast proteome with a movable ORF collection. Genes Dev. 19: 2816–2826. https://doi.org/10.1101/gad.1362105

Giaever, G., A. M. Chu, L. Ni, C. Connelly, L. Riles *et al.*, 2002 Functional profiling of the Saccharomyces cerevisiae genome. Nature 418: 387–391. https://doi.org/10.1038/nature00935

Gietz, R. D., 2014 Yeast transformation by the LiAc/SS carrier DNA/PEG method. Methods Mol. Biol. 1205: 1–12. https://doi.org/10.1007/978-1-4939-1363-3_1

Gimeno, C. J., and G. R. Fink, 1994 Induction of pseudohyphal growth by overexpression of PHD1, a Saccharomyces cerevisiae gene related to transcriptional regulators of fungal development. Mol. Cell. Biol. 14: 2100–2112. https://doi.org/10.1128/MCB.14.3.2100

Gimeno, C. J., P. O. Ljungdahl, C. A. Styles, and G. R. Fink, 1992 Unipolar cell divisions in the yeast S. cerevisiae lead to filamentous growth: regulation by starvation and RAS. Cell 68: 1077–1090. https://doi.org/10.1016/0092-8674(92)90079-R

González, B., A. Mas, G. Beltran, P. J. Cullen, and M. J. Torija, 2017 Role of mitochondrial retrograde pathway in regulating ethanol-inducible filamentous growth in yeast. Front. Physiol. 8: 148. https://doi.org/10.3389/fphys.2017.00148

Granek, J. A., and P. M. Magwene, 2010 Environmental and genetic determinants of colony morphology in yeast. PLoS Genet. 6: e1000823. https://doi.org/10.1371/journal.pgen.1000823

Greig, D., and M. Travisano, 2004 The Prisoner's Dilemma and polymorphism in yeast SUC genes. Proc. Biol. Sci. 271: S25–S26. https://doi.org/10.1098/rsbl.2003.0083

Guo, B., C. A. Styles, Q. Feng, and G. R. Fink, 2000 A Saccharomyces gene family involved in invasive growth, cell-cell adhesion, and mating. Proc. Natl. Acad. Sci. USA 97: 12158–12163. https://doi.org/10.1073/pnas.220420397

Hadwiger, J. A., C. Wittenberg, H. E. Richardson, M. de Barros Lopes, and S. I. Reed, 1989 A family of cyclin homologs that control the G1 phase in yeast. Proc. Natl. Acad. Sci. USA 86: 6255–6259. https://doi.org/10.1073/pnas.86.16.6255

Halme, A., S. Bumgarner, C. Styles, and G. R. Fink, 2004 Genetic and epigenetic regulation of the FLO gene family generates cell-surface variation in yeast. Cell 116: 405–415. https://doi.org/10.1016/S0092-8674(04)00118-7

Hamada, K., H. Terashima, M. Arisawa, N. Yabuki, and K. Kitada, 1999 Amino acid residues in the omega-minus region participate in cellular localization of yeast glycosylphosphatidylinositol-attached proteins. J. Bacteriol. 181: 3886–3889. https://doi.org/10.1128/JB.181.13.3886-3889.1999

Harbison, C. T., D. B. Gordon, T. I. Lee, N. J. Rinaldi, K. D. Macisaac *et al.*, 2004 Transcriptional regulatory code of a eukaryotic genome. Nature 431: 99–104. https://doi.org/10.1038/nature02800

Heise, B., J. van der Felden, S. Kern, M. Malcher, S. Bruckner *et al.*, 2010 The TEA transcription factor Tec1 confers promoter-specific gene regulation by Ste12-dependent and -independent mechanisms. Eukaryot. Cell 9: 514–531. https://doi.org/10.1128/EC.00251-09

Hohmann, S., 2002 Osmotic stress signaling and osmoadaptation in yeasts. Microbiol. Mol. Biol. Rev. 66: 300–372. https://doi.org/10.1128/MMBR.66.2.300-372.2002

Jarvis, E. E., D. C. Hagen, and G. F. Sprague, Jr., 1988 Identification of a DNA segment that is necessary and sufficient for alpha-specific gene control in Saccharomyces cerevisiae: implications for regulation of alpha-specific and a-specific genes. Mol. Cell. Biol. 8: 309–320. https://doi.org/10.1128/MCB.8.1.309

Kabir, M. A., M. A. Hussain, and Z. Ahmad, 2012 Candida albicans: a model organism for studying fungal pathogens. ISRN Microbiol. 2012: 538694. https://doi.org/10.5402/2012/538694

Karunanithi, S., and P. J. Cullen, 2012 The filamentous growth MAPK pathway responds to glucose starvation through the mig1/2 transcriptional repressors in Saccharomyces cerevisiae. Genetics 192: 869–887. https://doi.org/10.1534/genetics.112.142661

Karunanithi, S., N. Vadaie, C. A. Chavel, B. Birkaya, J. Joshi *et al.*, 2010 Shedding of the mucin-like flocculin Flo11p reveals a new aspect of fungal adhesion regulation. Curr. Biol. 20: 1389–1395. https://doi.org/10.1016/j.cub.2010.06.033

Karunanithi, S., J. Joshi, C. Chavel, B. Birkaya, L. Grell *et al.*, 2012 Regulation of mat responses by a differentiation MAPK pathway in Saccharomyces cerevisiae. PLoS One 7: e32294. https://doi.org/10.1371/journal.pone.0032294

Kennedy, M. J., A. L. Rogers, and R. J. Yancey, Jr., 1989 Environmental alteration and phenotypic regulation of Candida albicans adhesion to plastic. Infect. Immun. 57: 3876–3881. https://doi.org/10.1128/IAI.57.12.3876-3881.1989

Kim, J. H., and S. Powers, 1991 Overexpression of RPI1, a novel inhibitor of the yeast Ras-cyclic AMP pathway, down-regulates normal but not mutationally activated ras function. Mol. Cell. Biol. 11: 3894–3904. https://doi.org/10.1128/MCB.11.8.3894

Kim, K. Y., and D. E. Levin, 2010 Transcriptional reporters for genes activated by cell wall stress through a non-catalytic mechanism involving Mpk1 and SBF. Yeast 27: 541–548. https://doi.org/10.1002/yea.1782

King, L., and G. Butler, 1998 Ace2p, a regulator of CTS1 (chitinase) expression, affects pseudohyphal production in Saccharomyces cerevisiae. Curr. Genet. 34: 183–191. https://doi.org/10.1007/s002940050384

Kondo, K., and M. Inouye, 1991 TIP 1, a cold shock-inducible gene of Saccharomyces cerevisiae. J. Biol. Chem. 266: 17537–17544.

Koschwanez, J. H., K. R. Foster, and A. W. Murray, 2011 Sucrose utilization in budding yeast as a model for the origin of undifferentiated multicellularity. PLoS Biol. 9: e1001122. https://doi.org/10.1371/journal.pbio.1001122

Kraushaar, T., S. Bruckner, M. Veelders, D. Rhinow, F. Schreiner *et al.*, 2015 Interactions by the fungal Flo11 adhesin depend on a fibronectin type III-like adhesin domain girdled by aromatic bands. Structure 23: 1005–1017. https://doi.org/10.1016/j.str.2015.03.021

Kron, S. J., C. A. Styles, and G. R. Fink, 1994 Symmetric cell division in pseudohyphae of the yeast Saccharomyces cerevisiae. Mol. Biol. Cell 5: 1003–1022. https://doi.org/10.1091/mbc.5.9.1003

Kuchin, S., V. K. Vyas, and M. Carlson, 2002 Snf1 protein kinase and the repressors Nrg1 and Nrg2 regulate FLO11, haploid invasive growth, and diploid pseudohyphal differentiation. Mol. Cell. Biol. 22: 3994–4000. https://doi.org/10.1128/MCB.22.12.3994-4000.2002

Labbaoui, H., S. Bogliolo, V. Ghugtyal, N. V. Solis, S. G. Filler *et al.*, 2017 Role of Arf GTPases in fungal morphogenesis and virulence. PLoS Pathog. 13: e1006205. https://doi.org/10.1371/journal.ppat.1006205

Laloux, I., E. Dubois, M. Dewerchin, and E. Jacobs, 1990 TEC1, a gene involved in the activation of Ty1 and Ty1-mediated gene expression in Saccharomyces cerevisiae: cloning and molecular analysis. Mol. Cell. Biol. 10: 3541–3550. https://doi.org/10.1128/MCB.10.7.3541

Lamb, T. M., and A. P. Mitchell, 2003 The transcription factor Rim101p governs ion tolerance and cell differentiation by direct repression of the regulatory genes NRG1 and SMP1 in Saccharomyces cerevisiae. Mol. Cell. Biol. 23: 677–686. https://doi.org/10.1128/MCB.23.2.677-686.2003

Lambrechts, M. G., F. F. Bauer, J. Marmur, and I. S. Pretorius, 1996 Muc1, a mucin-like protein that is regulated by Mss10, is critical for pseudohyphal differentiation in yeast. Proc. Natl. Acad. Sci. USA 93: 8419–8424. https://doi.org/10.1073/pnas.93.16.8419

Lee, M. J., and H. G. Dohlman, 2008 Coactivation of G protein signaling by cell-surface receptors and an intracellular exchange factor. Curr. Biol. 18: 211–215. https://doi.org/10.1016/j.cub.2008.01.007

Lefrançois, P., G. M. Euskirchen, R. K. Auerbach, J. Rozowsky, T. Gibson *et al.*, 2009 Efficient yeast ChIP-Seq using multiplex short-read DNA sequencing. BMC Genomics 10: 37. https://doi.org/10.1186/1471-2164-10-37

Lenhart, B. A., B. Meeks, and H. A. Murphy, 2019 Variation in filamentous growth and response to quorum-sensing compounds in environmental isolates of Saccharomyces cerevisiae. G3 (Bethesda) 9: 1533–1544. https://doi.org/10.1534/g3.119.400080

Linder, T., and C. M. Gustafsson, 2008 Molecular phylogenetics of ascomycotal adhesins–a novel family of putative cell-surface adhesive proteins in fission yeasts. Fungal Genet. Biol. 45: 485–497. https://doi.org/10.1016/j.fgb.2007.08.002

Lipke, P. N., 2018 What we do not know about fungal cell adhesion molecules. J. Fungi (Basel) 4: 59. https://doi.org/10.3390/jof4020059

Liu, H., C. A. Styles, and G. R. Fink, 1993 Elements of the yeast pheromone response pathway required for filamentous growth of diploids. Science 262: 1741–1744. https://doi.org/10.1126/science.8259520

Lo, H. J., J. R. Kohler, B. DiDomenico, D. Loebenberg, A. Cacciapuoti *et al.*, 1997 Nonfilamentous C. albicans mutants are avirulent. Cell 90: 939–949. https://doi.org/10.1016/S0092-8674(00)80358-X

Lo, W. S., and A. M. Dranginis, 1996 FLO11, a yeast gene related to the STA genes, encodes a novel cell surface flocculin. J. Bacteriol. 178: 7144–7151. https://doi.org/10.1128/JB.178.24.7144-7151.1996

Lo, W. S., and A. M. Dranginis, 1998 The cell surface flocculin Flo11 is required for pseudohyphae formation and invasion by Saccharomyces cerevisiae. Mol. Biol. Cell 9: 161–171. https://doi.org/10.1091/mbc.9.1.161

Loeb, J. D., T. A. Kerentseva, T. Pan, M. Sepulveda-Becerra, and H. Liu, 1999 Saccharomyces cerevisiae G1 cyclins are differentially involved in invasive and pseudohyphal growth independent of the filamentation mitogen-activated protein kinase pathway. Genetics 153: 1535–1546.

Lorenz, M. C., and J. Heitman, 1998 The MEP2 ammonium permease regulates pseudohyphal differentiation in Saccharomyces cerevisiae. EMBO J. 17: 1236–1247. https://doi.org/10.1093/emboj/17.5.1236

Madhani, H. D., T. Galitski, E. S. Lander, and G. R. Fink, 1999 Effectors of a developmental mitogen-activated protein kinase cascade revealed by expression signatures of signaling mutants. Proc. Natl. Acad. Sci. USA 96: 12530–12535. https://doi.org/10.1073/pnas.96.22.12530

Meem, M. H., and P. J. Cullen, 2012 The impact of protein glycosylation on Flo11-dependent adherence in Saccharomyces cerevisiae. FEMS Yeast Res. 12: 809–818. https://doi.org/10.1111/j.1567-1364.2012.00832.x

Miller, K. Y., J. Wu, and B. L. Miller, 1992 StuA is required for cell pattern formation in Aspergillus. Genes Dev. 6: 1770–1782. https://doi.org/10.1101/gad.6.9.1770

Morrison, D. K., 2012 MAP kinase pathways. Cold Spring Harb. Perspect. Biol. 4: a011254. https://doi.org/10.1101/cshperspect.a011254

Mosch, H. U., R. L. Roberts, and G. R. Fink, 1996 Ras2 signals via the Cdc42/Ste20/mitogen-activated protein kinase module to induce filamentous growth in Saccharomyces cerevisiae. Proc. Natl. Acad. Sci. USA 93: 5352–5356. https://doi.org/10.1073/pnas.93.11.5352

Mutlu, N., D. T. Sheidy, A. Hsu, H. S. Jeong, K. J. Wozniak *et al.*, 2019 A stress-responsive signaling network regulating pseudohyphal growth and ribonucleoprotein granule abundance in Saccharomyces cerevisiae. Genetics 213: 705–720. https://doi.org/10.1534/genetics.119.302538

Ni, L., and M. Snyder, 2001 A genomic study of the bipolar bud site selection pattern in Saccharomyces cerevisiae. Mol. Biol. Cell 12: 2147–2170. https://doi.org/10.1091/mbc.12.7.2147

Nobile, C. J., J. E. Nett, D. R. Andes, and A. P. Mitchell, 2006 Function of Candida albicans adhesin Hwp1 in biofilm formation. Eukaryot. Cell 5: 1604–1610. https://doi.org/10.1128/EC.00194-06

Norman, K. L., C. A. Shively, A. J. De La Rocha, N. Mutlu, S. Basu *et al.*, 2018 Inositol polyphosphates regulate and predict yeast pseudohyphal growth phenotypes. PLoS Genet. 14: e1007493. https://doi.org/10.1371/journal.pgen.1007493

Olson, K. A., C. Nelson, G. Tai, W. Hung, C. Yong *et al.*, 2000 Two regulators of Ste12p inhibit pheromone-responsive transcription

by separate mechanisms. Mol. Cell. Biol. 20: 4199–4209. https://doi.org/10.1128/MCB.20.12.4199-4209.2000

Pan, X., and J. Heitman, 1999 Cyclic AMP-dependent protein kinase regulates pseudohyphal differentiation in Saccharomyces cerevisiae. Mol. Cell. Biol. 19: 4874–4887. https://doi.org/10.1128/MCB.19.7.4874

Pan, X., and J. Heitman, 2000 Sok2 regulates yeast pseudohyphal differentiation via a transcription factor cascade that regulates cell-cell adhesion. Mol. Cell. Biol. 20: 8364–8372. https://doi.org/10.1128/MCB.20.22.8364-8372.2000

Pan, X., and J. Heitman, 2002 Protein kinase A operates a molecular switch that governs yeast pseudohyphal differentiation. Mol. Cell. Biol. 22: 3981–3993. https://doi.org/10.1128/MCB.22.12.3981-3993.2002

Parachin, N. S., O. Bengtsson, B. Hahn-Hagerdal, and M. F. Gorwa-Grauslund, 2010 The deletion of YLR042c improves ethanolic xylose fermentation by recombinant Saccharomyces cerevisiae. Yeast 27: 741–751. https://doi.org/10.1002/yea.1777

Park, S. H., S. S. Koh, J. H. Chun, H. J. Hwang, and H. S. Kang, 1999 Nrg1 is a transcriptional repressor for glucose repression of STA1 gene expression in Saccharomyces cerevisiae. Mol. Cell. Biol. 19: 2044–2050. https://doi.org/10.1128/MCB.19.3.2044

Pitoniak, A., B. Birkaya, H. M. Dionne, N. Vadaie, and P. J. Cullen, 2009 The signaling mucins Msb2 and Hkr1 differentially regulate the filamentation mitogen-activated protein kinase pathway and contribute to a multimodal response. Mol. Biol. Cell 20: 3101–3114. https://doi.org/10.1091/mbc.e08-07-0760

Puria, R., M. A. Mannan, R. Chopra-Dewasthaly, and K. Ganesan, 2009 Critical role of RPI1 in the stress tolerance of yeast during ethanolic fermentation. FEMS Yeast Res. 9: 1161–1171. https://doi.org/10.1111/j.1567-1364.2009.00549.x

Reynolds, T. B., 2018 Going with the flo: the role of flo11-dependent and independent interactions in yeast Mat formation. J. Fungi (Basel) 4: 132. https://doi.org/10.3390/jof4040132

Reynolds, T. B., and G. R. Fink, 2001 Bakers' yeast, a model for fungal biofilm formation. Science 291: 878–881. https://doi.org/10.1126/science.291.5505.878

Roberts, C. J., B. Nelson, M. J. Marton, R. Stoughton, M. R. Meyer *et al.*, 2000 Signaling and circuitry of multiple MAPK pathways revealed by a matrix of global gene expression profiles. Science 287: 873–880. https://doi.org/10.1126/science.287.5454.873

Roberts, R. L., and G. R. Fink, 1994 Elements of a single MAP kinase cascade in Saccharomyces cerevisiae mediate two developmental programs in the same cell type: mating and invasive growth. Genes Dev. 8: 2974–2985. https://doi.org/10.1101/gad.8.24.2974

Robertson, L. S., and G. R. Fink, 1998 The three yeast A kinases have specific signaling functions in pseudohyphal growth. Proc. Natl. Acad. Sci. USA 95: 13783–13787. https://doi.org/10.1073/pnas.95.23.13783

Rodrigues, C. F., S. Silva, and M. Henriques, 2014 Candida glabrata: a review of its features and resistance. Eur. J. Clin. Microbiol. Infect. Dis. 33: 673–688. https://doi.org/10.1007/s10096-013-2009-3

Roumanie, O., C. Weinachter, I. Larrieu, M. Crouzet, and F. Doignon, 2001 Functional characterization of the Bag7, Lrg1 and Rgd2 RhoGAP proteins from Saccharomyces cerevisiae. FEBS Lett. 506: 149–156. https://doi.org/10.1016/S0014-5793(01)02906-4

Rupp, S., E. Summers, H. J. Lo, H. Madhani, and G. Fink, 1999 MAP kinase and cAMP filamentation signaling pathways converge on the unusually large promoter of the yeast FLO11 gene. EMBO J. 18: 1257–1269. https://doi.org/10.1093/emboj/18.5.1257

Ryan, O., R. S. Shapiro, C. F. Kurat, D. Mayhew, A. Baryshnikova *et al.*, 2012 Global gene deletion analysis exploring yeast filamentous growth. Science 337: 1353–1356. https://doi.org/10.1126/science.1224339

Sabbagh, Jr., W., L. J. Flatauer, A. J. Bardwell, and L. Bardwell, 2001 Specificity of MAP kinase signaling in yeast differentiation involves transient *vs.* sustained MAPK activation. Mol. Cell 8: 683–691. https://doi.org/10.1016/S1097-2765(01)00322-7

Schmitz, H. P., A. Jendretzki, C. Sterk, and J. J. Heinisch, 2018 The small yeast GTPase Rho5 and its dimeric GEF dck1/Lmo1 respond to glucose starvation. Int. J. Mol. Sci. 19: 2186. https://doi.org/10.3390/ijms19082186

Seger, R., 2010 *MAP Kinase Signaling Protocols*. Humana Press, New York. https://doi.org/10.1007/978-1-60761-795-2

Seger, R., and E. G. Krebs, 1995 The MAPK signaling cascade. FASEB J. 9: 726–735. https://doi.org/10.1096/fasebj.9.9.7601337

Sheppard, D. C., M. R. Yeaman, W. H. Welch, Q. T. Phan, Y. Fu *et al.*, 2004 Functional and structural diversity in the Als protein family of Candida albicans. J. Biol. Chem. 279: 30480–30489. https://doi.org/10.1074/jbc.M401929200

Sikorski, R. S., and P. Hieter, 1989 A system of shuttle vectors and yeast host strains designed for efficient manipulation of DNA in Saccharomyces cerevisiae. Genetics 122: 19–27.

Silva-Dias, A., I. M. Miranda, J. Branco, M. Monteiro-Soares, C. Pina-Vaz *et al.*, 2015 Adhesion, biofilm formation, cell surface hydrophobicity, and antifungal planktonic susceptibility: relationship among Candida spp. Front. Microbiol. 6: 205. https://doi.org/10.3389/fmicb.2015.00205

Singh, K., P. J. Kang, and H. O. Park, 2008 The Rho5 GTPase is necessary for oxidant-induced cell death in budding yeast. Proc. Natl. Acad. Sci. USA 105: 1522–1527. https://doi.org/10.1073/pnas.0707359105

Singh, K., M. E. Lee, M. Entezari, C. H. Jung, Y. Kim *et al.*, 2019 Genome-wide studies of rho5-interacting proteins that are involved in oxidant-induced cell death in budding yeast. G3 (Bethesda) 9: 921–931.

Smukalla, S., M. Caldara, N. Pochet, A. Beauvais, S. Guadagnini *et al.*, 2008 FLO1 is a variable green beard gene that drives biofilm-like cooperation in budding yeast. Cell 135: 726–737. https://doi.org/10.1016/j.cell.2008.09.037

Sobering, A. K., U. S. Jung, K. S. Lee, and D. E. Levin, 2002 Yeast Rpi1 is a putative transcriptional regulator that contributes to preparation for stationary phase. Eukaryot. Cell 1: 56–65. https://doi.org/10.1128/EC.1.1.56-65.2002

Sohn, K., J. Schwenk, C. Urban, J. Lechner, M. Schweikert *et al.*, 2006 Getting in touch with Candida albicans: the cell wall of a fungal pathogen. Curr. Drug Targets 7: 505–512. https://doi.org/10.2174/138945006776359395

Song, W., and M. Carlson, 1998 Srb/mediator proteins interact functionally and physically with transcriptional repressor Sfl1. EMBO J. 17: 5757–5765. https://doi.org/10.1093/emboj/17.19.5757

Spor, A., S. Wang, C. Dillmann, D. de Vienne, and D. Sicard, 2008 "Ant" and "grasshopper" life-history strategies in Saccharomyces cerevisiae. PLoS One 3: e1579. https://doi.org/10.1371/journal.pone.0001579

Stoldt, V. R., A. Sonneborn, C. E. Leuker, and J. F. Ernst, 1997 Efg1p, an essential regulator of morphogenesis of the human pathogen Candida albicans, is a member of a conserved class of bHLH proteins regulating morphogenetic processes in fungi. EMBO J. 16: 1982–1991. https://doi.org/10.1093/emboj/16.8.1982

Taheri, N., T. Kohler, G. H. Braus, and H. U. Mosch, 2000 Asymmetrically localized Bud8p and Bud9p proteins control yeast cell polarity and development. EMBO J. 19: 6686–6696. https://doi.org/10.1093/emboj/19.24.6686

Takahashi-Nakaguchi, A., K. Sakai, H. Takahashi, D. Hagiwara, T. Toyotome *et al.*, 2018 Aspergillus fumigatus adhesion factors

in dormant conidia revealed through comparative phenotypic and transcriptomic analyses. Cell. Microbiol. 20: e12802. https://doi.org/10.1111/cmi.12802

Tan, Z., M. Hays, G. A. Cromie, E. W. Jeffery, A. C. Scott *et al.*, 2013 Aneuploidy underlies a multicellular phenotypic switch. Proc. Natl. Acad. Sci. USA 110: 12367–12372. https://doi.org/10.1073/pnas.1301047110

Tedford, K., S. Kim, D. Sa, K. Stevens, and M. Tyers, 1997 Regulation of the mating pheromone and invasive growth responses in yeast by two MAP kinase substrates. Curr. Biol. 7: 228–238. https://doi.org/10.1016/S0960-9822(06)00118-7

Tkach, J. M., A. Yimit, A. Y. Lee, M. Riffle, M. Costanzo *et al.*, 2012 Dissecting DNA damage response pathways by analysing protein localization and abundance changes during DNA replication stress. Nat. Cell Biol. 14: 966–976. https://doi.org/10.1038/ncb2549

Tronchin, G., J. P. Bouchara, V. Annaix, R. Robert, and J. M. Senet, 1991 Fungal cell adhesion molecules in Candida albicans. Eur. J. Epidemiol. 7: 23–33. https://doi.org/10.1007/BF00221338

Vadaie, N., H. Dionne, D. S. Akajagbor, S. R. Nickerson, D. J. Krysan *et al.*, 2008 Cleavage of the signaling mucin Msb2 by the aspartyl protease Yps1 is required for MAPK activation in yeast. J. Cell Biol. 181: 1073–1081. https://doi.org/10.1083/jcb.200704079

van der Felden, J., S. Weisser, S. Bruckner, P. Lenz, and H. U. Mosch, 2014 The transcription factors Tec1 and Ste12 interact with coregulators Msa1 and Msa2 to activate adhesion and multicellular development. Mol. Cell. Biol. 34: 2283–2293. https://doi.org/10.1128/MCB.01599-13

Veelders, M., S. Bruckner, D. Ott, C. Unverzagt, H. U. Mosch *et al.*, 2010 Structural basis of flocculin-mediated social behavior in yeast. Proc. Natl. Acad. Sci. USA 107: 22511–22516. https://doi.org/10.1073/pnas.1013210108

Verstrepen, K. J., G. Derdelinckx, H. Verachtert, and F. R. Delvaux, 2003 Yeast flocculation: what brewers should know. Appl. Microbiol. Biotechnol. 61: 197–205. https://doi.org/10.1007/s00253-002-1200-8

Ward, M. P., C. J. Gimeno, G. R. Fink, and S. Garrett, 1995 SOK2 may regulate cyclic AMP-dependent protein kinase-stimulated growth and pseudohyphal development by repressing transcription. Mol. Cell. Biol. 15: 6854–6863. https://doi.org/10.1128/MCB.15.12.6854

Wendland, J., 2001 Comparison of morphogenetic networks of filamentous fungi and yeast. Fungal Genet. Biol. 34: 63–82. https://doi.org/10.1006/fgbi.2001.1290

White, M. A., L. Riles, and B. A. Cohen, 2009 A systematic screen for transcriptional regulators of the yeast cell cycle. Genetics 181: 435–446. https://doi.org/10.1534/genetics.108.098145

Wolfe, K. H., and D. C. Shields, 1997 Molecular evidence for an ancient duplication of the entire yeast genome. Nature 387: 708–713. https://doi.org/10.1038/42711

Younes, S., W. Bahnan, H. I. Dimassi, and R. A. Khalaf, 2011 The Candida albicans Hwp2 is necessary for proper adhesion, biofilm formation and oxidative stress tolerance. Microbiol. Res. 166: 430–436. https://doi.org/10.1016/j.micres.2010.08.004

Zahner, J. E., H. A. Harkins, and J. R. Pringle, 1996 Genetic analysis of the bipolar pattern of bud site selection in the yeast Saccharomyces cerevisiae. Mol. Cell. Biol. 16: 1857–1870. https://doi.org/10.1128/MCB.16.4.1857

Zeitlinger, J., I. Simon, C. T. Harbison, N. M. Hannett, T. L. Volkert *et al.*, 2003 Program-specific distribution of a transcription factor dependent on partner transcription factor and MAPK signaling. Cell 113: 395–404. https://doi.org/10.1016/S0092-8674(03)00301-5

Zhao, S., J. J. Huang, X. Sun, X. Huang, S. Fu *et al.*, 2018 (1-aryloxy-2-hydroxypropyl)-phenylpiperazine derivatives suppress Candida albicans virulence by interfering with morphological transition. Microb. Biotechnol. 11: 1080–1089. https://doi.org/10.1111/1751-7915.13307

Zheng, W., H. Zhao, E. Mancera, L. M. Steinmetz, and M. Snyder, 2010 Genetic analysis of variation in transcription factor binding in yeast. Nature 464: 1187–1191. https://doi.org/10.1038/nature08934

Zhou, H., and F. Winston, 2001 NRG1 is required for glucose repression of the SUC2 and GAL genes of Saccharomyces cerevisiae. BMC Genet. 2: 5. https://doi.org/10.1186/1471-2156-2-5

Zhou, W., M. W. Dorrity, K. L. Bubb, C. Queitsch, and S. Fields, 2020 Binding and regulation of transcription by yeast Ste12 variants to drive mating and invasion phenotypes. Genetics 214: 397–407. https://doi.org/10.1534/genetics.119.302929

Communicating editor: A. Gladfelter